REDUCTION OF PHOTOGRAPHIC HEAT-TRANSFER RATE DATA AT AEDC

R. K. Matthews and G. E. Gilley

ARO, Inc.

June 1973

VON KÁRMÁN GAS DYNAMICS FACILITY
ARNOLD ENGINEERING DEVELOPMENT CENTER
AIR FORCE SYSTEMS COMMAND
ARNOLD AIR FORCE STATION, TENNESSEE

NOTICES

When U. S. Government drawings specifications, or other data are used for any purpose other than a definitely related Government procurement operation, the Government thereby incurs no responsibility nor any obligation whatsoever, and the fact that the Government may have formulated, furnished, or in any way supplied the said drawings, specifications, or other data, is not to be regarded by implication or otherwise, or in any manner licensing the holder or any other person or corporation, or conveying any rights or permission to manufacture, use, or sell any patented invention that may in any way be related thereto.

Qualified users may obtain copies of this report from the Defense Documentation Center.

References to named commercial products in this report are not to be considered in any sense as an endorsement of the product by the United States Air Force or the Government.

REDUCTION OF PHOTOGRAPHIC HEAT-TRANSFER RATE DATA AT AEDC

R. K. Matthews and G. E. Gilley
ARO, Inc.

FOREWORD

The work reported herein was conducted at the Arnold Engineering Development Center (AEDC), Air Force Systems Command (AFSC), Arnold Air Force Station, Tennessee.

The test results presented were obtained by ARO, Inc. (a subsidiary of Sverdrup & Parcel and Associates, Inc.), contract operator of AEDC, AFSC. The work was done under ARO Project No. VK008 to develop efficient and productive operating techniques. The time period was from July 1971 to September 1972. The manuscript was submitted for publication on March 19, 1973.

The authors wish to express their appreciation to Cord Link of the ARO, Inc., Central Computing Organization for his help with the photogrammetry aspects of this work and to Manual Brown of the VKF for the mechanical and electrical engineering work required in the development of this system.

This technical report has been reviewed and is approved.

JIMMY W. MULLINS
Lt Colonel, USAF
Chief Air Force Test Director, VKF
Directorate of Test

A. L. COAPMAN
Colonel, USAF
Director of Test

ABSTRACT

The development of the phase-change paint technique has provided access to a wealth of information in the form of photographs of heating rate patterns on wind tunnel test models. However, difficulty is experienced in the transformation of the data from the photographs to model coordinates because of the distortion of the model image caused by oblique camera views. This report documents the unique capabilities recently developed at the AEDC-VKF for transformation of the photographic information into a model axis system and for presentation of the data in machine generated plots.

To avoid extensive data reduction procedure obtain a tare photograph at each model attitude and each camera with a grid overlay on the area of interest.

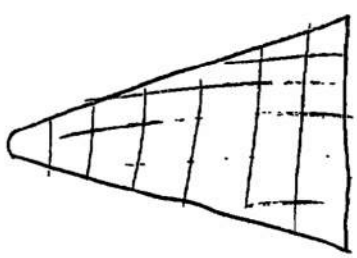

Tare

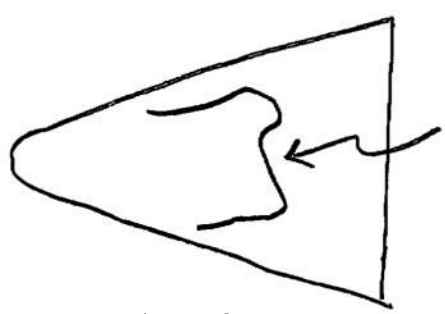

Melt line

then overlay each

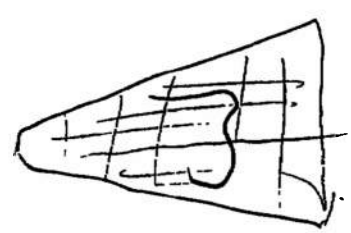

CONTENTS

APPENDIX
ILLUSTRATIONS

Figure

NOMENCLATURE

A B C D	Constants in transformation equations (Eq. 6)
c	Specific heat of model material, Btu/lbm-°R
f	Focal length of camera lens (see Fig. 11), in.
H(TO)	Heat-transfer coefficient based on $T_{aw} = T_o$
H(.9TO)	Heat-transfer coefficient based on $T_{aw} = 0.9T_o$
H(.85TO)	Heat-transfer coefficient based on $T_{aw} = 0.85T_o$
HREF	Reference heat-transfer coefficient, Btu/ft^2-sec-°R
h	Heat-transfer coefficient, Btu/ft^2-sec-°R
k	Thermal conductivity of model material, Btu/ft-sec-°R
L	Model length, in.
P_1, P_2, P_3, P_4	Points in u,v plane surrounding arbitrary point on melt line (see Fig. 13)
$P_{T_{R1}}, P_{T_{R2}}$	Reference points in tracing plane
S	Scale factor between $X_T Y_T$ plane and u,v plane (see Fig. 12)
T	Temperature, °R or °F as noted
t	Elapsed time from initial exposure of model to free-stream airflow, sec
u,v	Film plane coordinate system
(u_{R1}, v_{R1}) (u_{R2}, v_{R2})	Coordinates of reference points R1 and R2 in u,v plane
$(u_i v_i)$	u,v coordinates of the i^{th} model geometry point where i includes all model points
(u_p, v_p)	u,v coordinates of arbitrary point on melt line (see Fig. 13)
$(u_1, v_1)(u_2, v_2)$ $(u_3, v_3)(u_4, v_4)$	u,v coordinates of points surrounding arbitrary point on melt line (see Fig. 13)

V_{12}, V_{34}	Interpolated value of v between P_1P_2 and P_3P_4, respectively (Eq. 10 and 11)
W_x	Interpolation weight factor for x model coordinate (Eq. 9)
W_{u12}, W_{u34}	Interpolation weight factors between u_1, u_2 and u_3, u_4 (Eq. 12)
X_m, Y_m, Z_m	Model axis system (see Fig. 9)
$X_{m_m}, Y_{m_m}, Z_{m_m}$	Model surface coordinates in model axis system (see Fig. 9)
$X_c Y_c Z_c$	Camera axis system (see Fig. 11)
$X_{m_c}, Y_{m_c}, Z_{m_c}$	Coordinates of camera origin in model axis system
$X_{c_m}, Y_{c_m}, Z_{c_m}$	Coordinates of model surface in camera axis system after translation and rotation through ϕ and θ
X_T, Y_T	Tracing plane coordinate system (see Fig. 12)
$(X_{T_{R1}}, Y_{T_{R1}})$ $(X_{T_{R2}}, Y_{T_{R2}})$	Coordinates of reference points R1 and R2 in tracing (X_T, Y_T) plane (see Fig. 12)
$X_{m_{R1}}, Y_{m_{R1}}, Z_{m_{R1}}$ $X_{m_{R2}}, Y_{m_{R2}}, Z_{m_{R2}}$	Coordinates of reference points $P_{T_{R1}}$ and $P_{T_{R2}}$ in model axis system
X_{12}, X_{34}	Model X station containing points 1, 2 and 3, 4, respectively (see Figs. 9 and 13)
X_{m_1}, X_{m_2}, X_{m_3}, X_{m_4}	Model X coordinate of points 1, 2, 3, and 4
Y_{m_1}, Y_{m_2}, Y_{m_3}, Y_{m_4}	Model Y coordinate of points 1, 2, 3, and 4
Z_{m_1}, Z_{m_2}, Z_{m_3}, Z_{m_4}	Model Z coordinate of points 1, 2, 3, and 4
α	Model angle of attack, deg
β	Angle between Y_T axis and u axis (see Fig. 12), deg
θ	Elevation angle of camera line of sight relative to the X_m, Y_m plane (see Fig. 10), deg

ρ	Density of model material, lbm/ft^3
ϕ	Rotation angle about the Z_m axis (see Fig. 10), deg

TEMPERATURE SUBSCRIPTS

aw	Adiabatic wall
i	Initial temperature prior to exposure to airflow
o	Stagnation
pc	Phase change
w	Model wall

SECTION I
INTRODUCTION

Aerodynamic heating considerations played an important role in the design of the Mercury, Gemini, and Apollo vehicles. The Space Shuttle thermal protection system is typical of today's aerodynamic heating problems, and advanced interceptors and hypersonic transports represent the next generation of heating problems. Just as the configurations have become more sophisticated over the years, so have the testing techniques to handle these aerodynamic heating problems. Jones and Hunt (Ref. 1) pioneered development of the phase-change paint technique and Compton (Ref. 2) has documented preliminary heating results obtained by using an infrared camera. These thermal mapping techniques can provide a complete heating distribution on a given model surface. However, the transformation of the data to plots has been a drawback particularly in the case of phase-change paint data.

The basic phase-change paint data consist of sequenced photographs or motion-picture film which show the progression of the phase-change paint melt lines. Nossaman (Ref. 3) and Throckmorton (Ref. 4) discuss some of the difficulties in attempting to automate the transformation of the melt lines from the photographic plane to data plots. The staff of the VKF has been particularly concerned about the automation of the data reduction process because of the large volume of photographs generated during a typical test. For example, during a space shuttle orbiter reentry test (Ref. 5), three cameras were used to simultaneously photograph the top, side, and bottom model surfaces, and approximately 5000 photographs were obtained per day. Of these about 200 were used to extract heating data.

The purpose of this report is to document the procedures developed at the VKF to convert the information contained on phase-change paint photographs to machine-generated model axis data plots. The procedures previously employed consisted of overlaying a model grid and reading the coordinates of the melt line of a given photograph and then using charts to determine the corresponding value of the heat-transfer coefficient (for example, see Refs. 6 and 7). This technique is extremely tedious and time consuming if a significant number of data plots are required. However, it should be understood that in cases of complex model geometry the actual phase-change paint photograph may be the best way to present the data.

SECTION II
TEST PROCEDURES

The phase-change paint technique of measuring the heat transfer to a model surface was developed by Jones and Hunt (Ref. 1). This technique assumes that the model wall temperature response is similar to that of a semi-infinite slab subjected to an instantaneous and constant heat-transfer coefficient. The surface wall temperature rise for a semi-infinite slab is given by the equation

$$\frac{T_w - T_i}{T_{aw} - T_i} = 1 - e^{b^2} \operatorname{erfc} b \qquad (1)$$

where $b = h\sqrt{t}/\sqrt{\rho ck}$.

A specific value of the wall temperature (T_w) is indicated by a phase-change paint (Tempilaq®). These paints change from an opaque solid to a transparent liquid at a specified phase-change temperature (T_{pc}). For known values of T_i, T_{aw}, t, and $\sqrt{\rho ck}$, the heat-transfer coefficient (h) can be calculated as a function of the time required for the phase change to occur by using $T_w = T_{pc}$. That is,

$$h = \frac{b\sqrt{\rho ck}}{\sqrt{t}} \qquad (2)$$

where b comes from the solution of Eq. (1) since the left-hand side is known.

Prior to each run, the model is cleaned and cooled with alcohol and then spray painted with Tempilaq. In most cases, the windward and leeward surfaces are sprayed with different paints since the leeside surface temperatures are generally lower than the windward surface temperatures. The model is installed on the model injection mechanism at the desired test attitude, and the model initial temperature (T_i) is measured. The model is then injected into the airstream for approximately 25 sec and during this time the model surface temperature rise produces isotherm melt lines. The progression of the melt lines is photographed with 70-mm sequenced cameras operating at two frames per second. Typical examples of phase-change paint photographs obtained during a run are presented in Fig. 1 (Appendix), and a typical camera arrangement is illustrated in Fig. 2. Figure 3 illustrates the film plane distortion of a model caused by the oblique camera viewing angles and shows that linear scaling from photographs should be avoided.

During each run, the tunnel stagnation conditions and the time of each picture are recorded on magnetic tape as well as the model initial temperature and the phase-change paint temperature (T_{pc}). As previously mentioned, these parameters are used in the solution of Eq. (1) and provide a value of heat-transfer coefficient which is associated with each picture. A sample printout illustrating this phase of the data reduction technique is presented in Fig. 4. It should be emphasized that the basic information presented in Fig. 4 is simply a tabulation of the semi-infinite slab equation solution for various times. Of course, to be useful these calculated heat-transfer parameters must be associated with a melt line on the photograph obtained at a corresponding time. Also note that Fig. 4 includes heat-transfer coefficients calculated for assumed adiabatic wall temperatures of T_o, $0.9T_o$, and $0.85T_o$. The use of three values of T_{aw} provides an indication of the sensitivity of the heat-transfer coefficients to the value of T_{aw} assumed. As can be seen, there are large percentage differences in the values of the heat-transfer coefficients. Therefore, if the data are to be used for flight predictions, the value of T_{aw}/T_o is obviously very important.

SECTION III
DATA REDUCTION PROCEDURES

Plots illustrating typical axial and spanwise comparisons of data and theory are shown in Fig. 5. These types of plots are frequently the desired results of a phase-change paint test. Therefore, the problem is to convert the information from the phase-change paint photographs (Fig. 1) into heat-transfer rate distribution plots (Fig. 5). Figure 6 is a schematic of how this is done, and the sections that follow provide the details of the procedures. In general, the steps are:

1. Interpret and trace melt lines from photographs,
2. Record melt line coordinates on magnetic tape,
3. Mathematically transform the model coordinates into the film plane and overlay the melt line,
4. Interpolate to determine body coordinates of the melt line, and
5. Machine generate the desired data plots.

3.1 RECORDING MELT LINES

A film editing machine (Fig. 7) is used to review the 70-mm film obtained during the test. When the observer comes to a frame of interest he simply traces the melt contour on Mylar® film and records the picture frame number with the tracing. Since the determination of the proper melt line requires some judgment (Ref. 4), an engineer familiar with the test is needed to supervise or perform the task of making the melt line tracings. Experience has shown that the number of hours required to make the tracings is approximately equal to the wind tunnel hours required to obtain the photographs.

These melt line tracings and the corresponding reference points and frame numbers are recorded on magnetic tape by using an analog tracing system (Fig. 8).[1] The frame number links a value of heat-transfer coefficient (see Section II) with the picture plane coordinates of the melt lines and the reference points are used in scaling.

3.2 TRANSFORMATION OF MODEL COORDINATES TO FILM PLANE

The mechanics of the model coordinate transformation to the film plane require that the three-dimensional model coordinates which are recorded in the model axis system first be transformed into the camera axis system and then into the two-dimensional film plane coordinate system. A double subscript notation used to identify the axis systems and points is illustrated as follows:

[1]Experience has shown that it is more efficient to perform a two-step operation in recording the melt lines as opposed to going directly from the photographs to the magnetic tape.

X_{m_m}	X component model axis system model surface points
X_{m_c}	X component model axis system camera focal point
X_{c_m}	X component camera axis system model surface points

The model surface coordinates ($X_{m_m}, Y_{m_m}, Z_{m_m}$) are measured using a Sheffield Cordax measuring machine as illustrated in Fig. 9. The location of the camera focal point (X_{m_c}, Y_{m_c}, Z_{m_c}) and the camera line of sight are specified in the model axis system. The direction of the camera line of sight is defined by two angles (ϕ and θ), where ϕ is the rotation angle around the Z_m axis and θ is the elevation angle with respect to the $X_m Y_m$ plane. The z axis of the camera coordinate system is coincident with the camera line of sight (see Fig. 10).

Given the model coordinates and the camera parameters, each point on the model is transformed into the film plane, thereby constructing a mathematical "photograph" of the model (Fig. 11). That is, the three-dimensional model coordinates are transformed into a two-dimensional film plane coordinate system which is designated as the u,v plane. The mechanics of the transformation are outlined in the remainder of this section.

Each model surface point in the model axis system is translated and rotated to the camera coordinate system by the following transformation:

$$\begin{vmatrix} X_{c_m} \\ Y_{c_m} \\ Z_{c_m} \end{vmatrix} = \begin{vmatrix} -\sin\phi & \cos\phi & 0 \\ -\sin\theta\cos\phi & -\sin\theta\sin\phi & \cos\theta \\ \cos\theta\cos\phi & \cos\theta\sin\phi & \sin\theta \end{vmatrix} \begin{vmatrix} X_{m_m} - X_{m_c} \\ Y_{m_m} - Y_{m_c} \\ Z_{m_m} - Z_{m_c} \end{vmatrix} \tag{3}$$

Projection of these coordinates onto the film plane (u,v plane) is obtained by

$$u = f\left(\frac{X_{c_m}}{Z_{c_m}}\right) \qquad v = f\left(\frac{Y_{c_m}}{Z_{c_m}}\right) \tag{4}$$

where f is the distance from the focal point to the u,v plane. This distance is the same as the lens to film distance in the camera (Fig. 11).

There is now a set of (u,v) points for the set of model geometry points ($X_{m_m}, Y_{m_m}, Z_{m_m}$). The next step is to scale the melt line coordinates to this same u,v plane.

The melt line coordinates are recorded in the tracing plane as illustrated in Figs. 8 and 12. These coordinates must also be transformed onto the film plane before the model coordinates of the melt line can be determined.

In general, the transformation of a point from the tracing plane to the u,v plane is given by

$$\begin{aligned} u &= (S \cos \beta) Y_T + (S \sin \beta) X_T - C \\ v &= (S \cos \beta) X_T - (S \sin \beta) Y_T - D \end{aligned} \tag{5}$$

where the nomenclature is illustrated in Fig. 12. Letting $A = S \cos \beta$ and $B = S \sin \beta$ gives

$$\begin{aligned} u &= A Y_T + B X_T + C \\ v &= A X_T - B Y_T + D \end{aligned} \tag{6}$$

where A, B, C, and D are four unknowns, These unknown coefficients are solved for by using two known points called reference marks. The two reference marks are identified in the tracing plane (Fig. 12) as ($P_{T_{R1}}$, $P_{T_{R2}}$). The known model coordinates of these points are ($X_{m_{R1}}$, $Y_{m_{R1}}$, $Z_{m_{R1}}$) and ($X_{m_{R2}}$, $Y_{m_{R2}}$, $Z_{m_{R2}}$), and the tracing plane coordinates are ($X_{T_{R1}}$, $Y_{T_{R1}}$) and ($X_{T_{R2}}$, $Y_{T_{R2}}$). The model coordinates are transformed into the u,v plane by Eqs. (3) and (4) to give (u_{R1},v_{R1}) and (u_{R2},v_{R2}). Substitution into Eq. (6) gives

$$\begin{aligned} u_{R1} &= AY_{T_{R1}} - BX_{T_{R1}} + C \\ v_{R1} &= AX_{T_{R1}} - BY_{T_{R1}} + D \\ u_{R2} &= AY_{T_{R2}} - BX_{T_{R2}} + C \\ v_{R2} &= AX_{T_{R2}} - BY_{T_{R2}} + D \end{aligned} \tag{7}$$

The simultaneous solution of these equations for A, B, C, and D allows all points on the melt line to be transformed from the tracing plane to the u,v plane by applying Eq. (6) to each melt line point.

3.3 INTERPOLATION OF MELT LINE POINTS TO DETERMINE BODY COORDINATES

As described in the previous two sections, the points along the melt line and the model surface coordinates are transformed into the film plane axis system (u,v plane). The next step in the data reduction process is to interpolate in the u,v plane to determine the model coordinates (X_m, Y_m, Z_m) of the melt lines.

A search is made in the u,v plane to find the point (u_1,v_1) which is a minimum distance from the melt line point (u_p,v_p). That is, the minimum of

$$\sqrt{(u_p - u_i)^2 + (v_p - v_i)^2}$$

for all model geometry points is found (see Fig. 13). After the point P_1 is found, a search is made to find the second nearest point to the point (u_p,v_p). This point (P_2) is restricted to the same model station[2] as P_1 so that P_1 and P_2 both have the same X_m model coordinate which is designated, X_{12}. At a different model station, the third and fourth closest points to the melt line point are determined such that the melt line point falls within a quadrilateral as illustrated in Figs. 13 and 14a. The points P_3 and P_4 are also restricted such that they have the same value for the X_m model coordinate (designated X_{34}). Model station X_{34} is adjacent to model station X_{12}.

To determine the (X_m,Y_m,Z_m) model coordinates of the melt line point (u_p,v_p), a simple linear interpolation technique is applied which uses weighting factors. For example, since the unknown melt line point is inside the quadrilateral bounded by the model X_m coordinates (X_{12} and X_{34}), it is known that its X_m model coordinate has a value between X_{12} and X_{34}. A weighting factor (W_x) is calculated such that

W_x = 0 when v_p lies on the same model station as X_{m_1} and X_{m_2} (see Fig. 14b)

and

W_x = 1 when v_p lies on the same model station as X_{m_3} and X_{m_4}.

Then the X_m model coordinate of the unknown point is given by

$$X_m = X_{12} + (X_{34} - X_{12}) W_x \tag{8}$$

[2]As described at the beginning of this section, the model coordinates were recorded at constant model stations, and therefore, adjacent spanwise points have the same X_m model coordinate.

As illustrated in Fig. 14b the value of the weighting factor (W_x) goes from 0 to 1 depending on the magnitude of v_p. The factor W_x is calculated by the ratio:

$$W_x = \frac{v_p - V_{12}}{V_{34} - V_{12}} \tag{9}$$

where

$$V_{12} = v_1 + (v_2 - v_1)W_{u12} \qquad \text{(see Fig. 14c)} \tag{10}$$

and

$$V_{34} = v_3 + (v_4 - v_3)W_{u34} \tag{11}$$

As can be seen, the technique used to calculate V_{12} and V_{34} is similar to that used to calculate X_m (Eq. 8). The weighting factors (W_{u12} and W_{u34}) are given by the equations:

$$W_{u12} = \frac{u_p - u_1}{u_2 - u_1}$$

$$W_{u34} = \frac{u_p - u_3}{u_4 - u_3} \qquad \text{(see Fig. 14d)} \tag{12}$$

Note that; $W_{u12} = 0$ when $u_p = u_1$, and $W_{u12} = 1$ when $u_p = u_2$.

The procedure described above and illustrated in Fig. 14 is used to calculate the model X_m coordinate of an arbitrary point on the melt line. The procedure used to calculate the model Y_m coordinate of the melt line points is similar. The equations are:

$$Y_m = Y_{12} + (Y_{34} - Y_{12})W_x \qquad \text{(see Eq. 8)} \tag{13}$$

where

$$Y_{12} = Y_{m_1} + (Y_{m_2} - Y_{m_1})W_{u12} \tag{14}$$

and

$$Y_{34} = Y_{m_3} + (Y_{m_4} - Y_{m_3})W_{u34} \tag{15}$$

Substitution and simplification yield

$$\begin{aligned} Y_m = {} & Y_{m_1}(1 - W_{u12})(1 - W_x) \\ & + Y_{m_2}(W_{u12})(1 - W_x) \\ & + Y_{m_3}(W_x)(1 - W_{u34}) \\ & + Y_{m_4}(W_x)(W_{u34}) \end{aligned} \tag{16}$$

In a like manner, it can be shown that

$$\begin{aligned} Z_m = {} & Z_{m_1}(1 - W_{u12})(1 - W_x) \\ & + Z_{m_2}(W_{u12})(1 - W_x) \\ & + Z_{m_3}(W_x)(1 - W_{u34}) \\ & + Z_{m_4}(W_x)(W_{u34}) \end{aligned} \tag{17}$$

3.4 DATA PRESENTATION

With the model coordinates of a melt line and the corresponding heat-transfer coefficient stored on tape, the final step is to present the data in a convenient form. Several methods were considered before selection of the format illustrated in Fig. 15. Presented in Fig. 15[3] is the final data reduction of the run illustrated in Fig. 1. There are three parts to the final data presentation:

1. Figure 15a: tabulated heating parameters for each selected picture plus run conditions and model attitude.

2. Figure 15b to i: the model coordinates X_m, Y_m of the melt line for different levels of heating presented with a planform view of the model outline. Of course, for a side-mounted camera a side view of the model outline would be presented. It should be emphasized that the melt line (or heating level) coordinates are in the model axis system and do not include the distortion associated with a photograph.

3. Figure 15j: axial and spanwise data plots. Once the melt lines are transformed into the model coordinate system, it is relatively simple to machine generate this type of data plots.

SECTION IV
CONCLUDING REMARKS

The difficulty in converting heat-transfer-rate information from phase-change paint photographs to data plots has been a drawback to the phase-change paint technique. This report documents the unique capabilities recently developed at the AEDC-VKF for transforming the photographic information obtained from phase-change paint tests into a model axis system and then presentation of the data in machine-generated plots.

---

[3]This figure was taken directly from Ref. 8, and additional examples of AEDC-VKF reduced paint data may be found in Refs. 9 through 12.

The procedures described in this report deal with the specific problem of extracting information from phase-change paint photographs and correcting for camera viewing angle; however, it should be noted that many of these same procedures could be applied to extracting information from any photograph. For example, these procedures could be used on thermographic phosphor, shadowgraph, schlieren, and oil flow photographs.

REFERENCES

1. Jones, Robert A., and Hunt, James L. "Use of Fusible Temperature Indicators for Obtaining Quantitative Aerodynamic Heat-Transfer Data." NASA-TR-R-230, February 1966.

2. Compton, Dale L. "Convective Heating Measurement by Means of an Infrared Camera." NASA TMX-2507, February 1972.

3. Nossaman, G. O. "Feasibility Study for Automatic Reduction of Phase Change Imagery." NASA CR-112001, 1971.

4. Throckmorton, David A. "Heat-Transfer Testing Procedures in Phase B Shuttle Studies with Emphasis on Phase-Change-Data Improvement." NASA TMX-2507, February 1972.

5. Matthews, R. K., Eaves, R. H., and Martindale, W. R. "Heat-Transfer and Flow-Field Tests of the McDonnell Douglas–Martin Marietta Space Shuttle Configuration." AEDC-TR-73-53 (AD000000), April 1973.

6. Schmitt, D. A. "Thermal Mapping Investigation of a 0.325-Percent Scale MDC/MMC Phase B Booster Configuration with Ventral Tip Fins." DMS-DR-1138, July 1971.

7. Creel, T. R., Jr., Gorowitz, Harold, and Raparelli, Raymond. "Heat Transfer Verification on North American Rockwell Delta Wing Orbiter (SSV-161B)." DMS-DR-1165, August 1971.

8. Matthews, R. K., Martindale, W. R., Warmbrod, J. D., and Johnson, C. B. "Heat Transfer Investigation of Langley Research Center Transition Models at a Mach Number of 8." NASA CR-120,045, March 1972.

9. Matthews, R. K., Martindale, W. R., and Warmbrod, J. D. "Heat Transfer Rate Distributions on McDonnell Douglas Booster Determined by Phase Change Technique for Nominal Mach Number of 8." NASA CR-120,043, April 1972.

10. Matthews, R. K., Martindale, W. R., and Warmbrod, J. D. "Heat Transfer Rate Distributions on McDonnell Douglas Delta Wing Orbiter Determined by Phase-Change Paint Technique for Nominal Mach Number of 8." NASA CR-120,025, July 1972.

11. Matthews, R. K., Martindale, W. R., and Warmbrod, J. D. "Heat Transfer Rate Distribution on North American Rockwell Delta Wing Orbiter Determined by Phase Change Paint Technique at a Mach Number of 8." NASA CR-120,048, March 1972.

12. Taswala, M. D. and Stultz, J. W. "Wind Tunnel Investigation of Aerodynamic Heating and Transition Characteristics on an 80-deg Delta Wing Configuration." McDonnell Douglas Astronautics Company-East Report MDC E 0640, July 1972.

APPENDIX
ILLUSTRATIONS

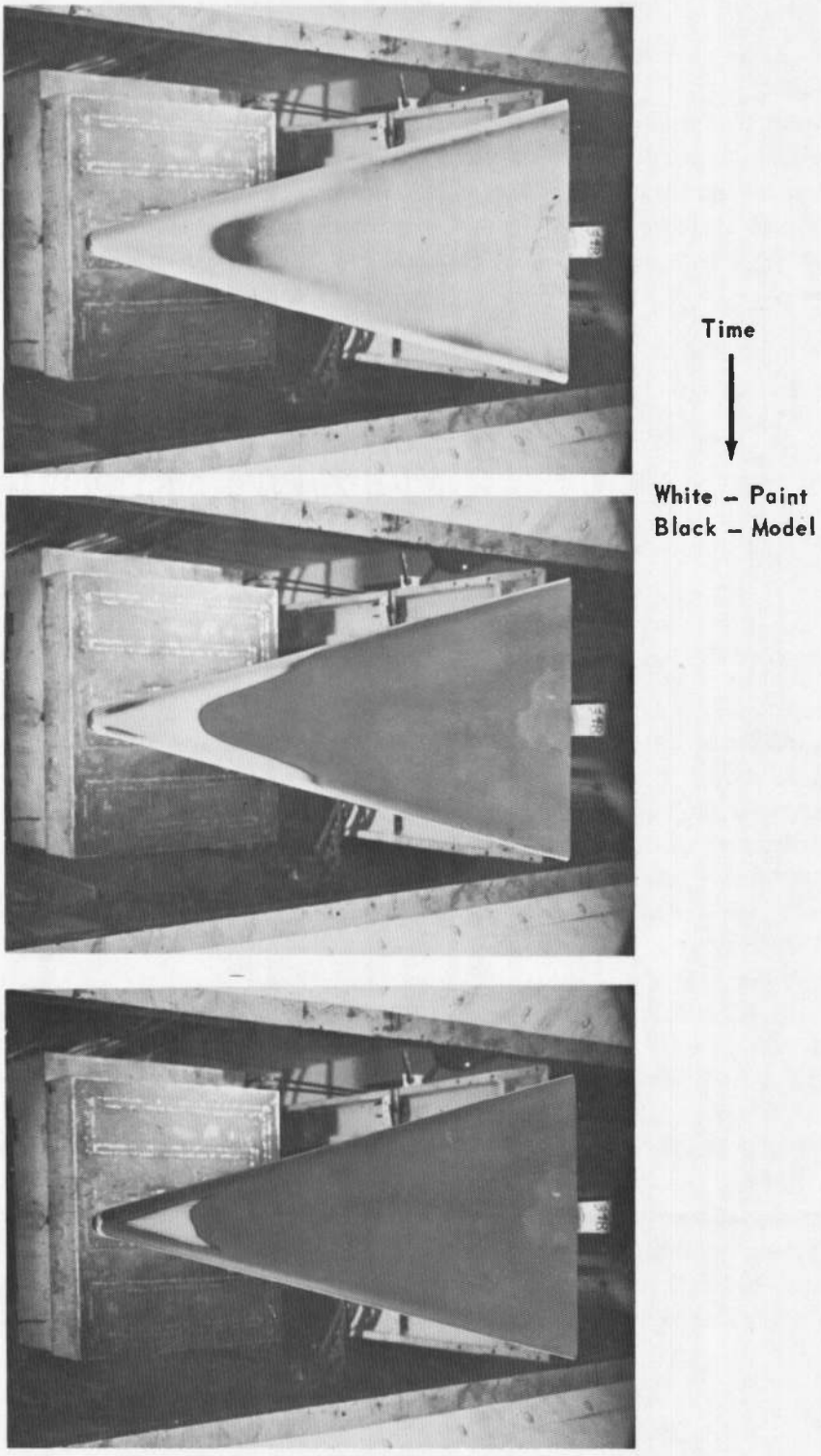

Fig. 1 Typical Examples of Phase-Change Paint Photographs

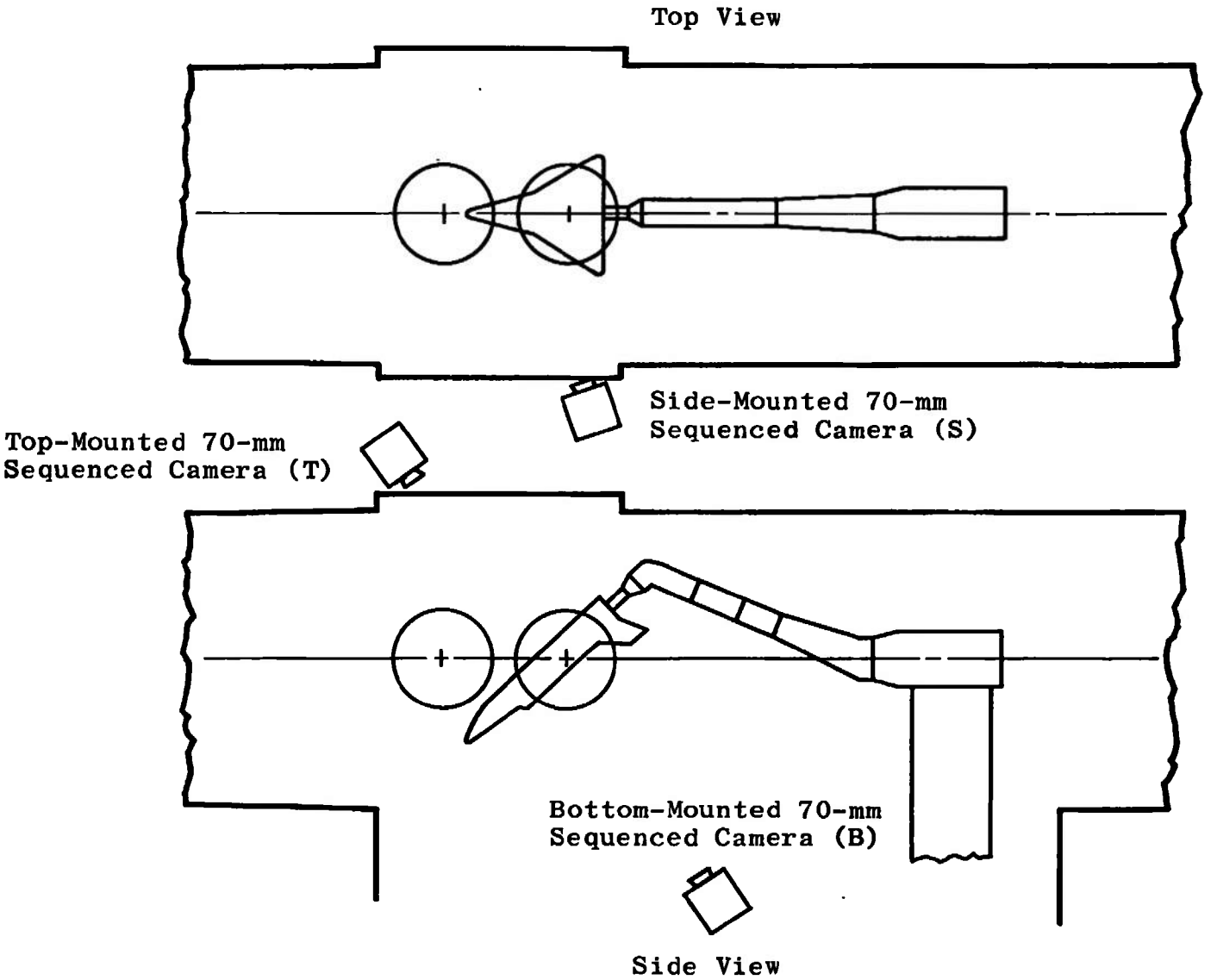

Fig. 2 Typical Installation for Phase-Change Paint Test

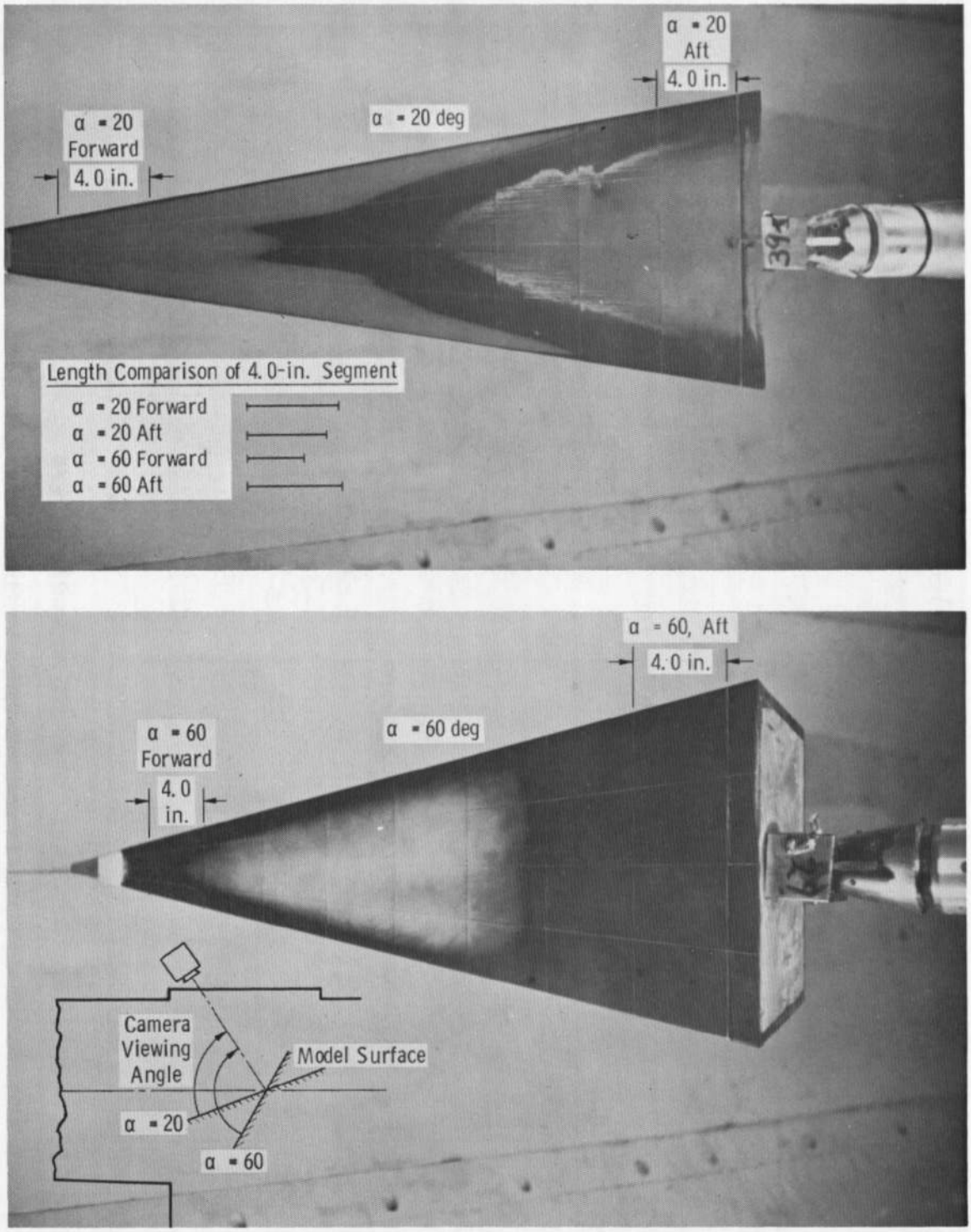

Fig. 3 Illustration of Model Distortion Caused by Camera Viewing Angle

MUST GET IN SEQUENCE WITH MELT LINES

GROUP	CONFIG	ALPHA-SECTOR	ALPHA-PREREND	ROLL-MODEL	ALPHA-MODEL	YAW	MACH NO	PO PSIA	TO DEG R
A	REENTRY	2.00	-31.80	180.00	29.80	.00	8.00	298.0	1263.5

T-INF (DEG R)	P-INF (PSIA)	Q-INF (PSIA)	V-INF (FT/SEC)	RHO-INF (SLUGS/FT3)	MU-INF (LB-SEC/FT2)	RE/FT (FT-1)	STFR (R= .0310 FT)
91.6	.0305	1.367	3751	2.80E-05	7.37E-08	1.42E 06	2.58E-02

PHASE CHANGE TEMP	INITIAL TEMP	SQUARE ROOT(RHO X C X K)
568 AND 685 DEG R	540 DEG R	3.67E-02
108 AND 225 DEG F	80 DEG F	

PICTURE NUMBER	TIME OFL	TIME	T AVG	H(TO)	ST(TO)	ST/STFR	H(.85TO)	ST(.85TO)	H(.90TO)	ST(.90TO)
5108	MODEL HAS NOT REACHED CENTERLINE									
9422	MODEL HAS NOT REACHED CENTERLINE									
3611	MODEL HAS NOT REACHED CENTERLINE									
5109	MODEL HAS NOT REACHED CENTERLINE									
9423	MODEL HAS NOT REACHED CENTERLINE									
3612	MODEL HAS NOT REACHED CENTERLINE									
5110	MODEL HAS NOT REACHED CENTERLINE									
9424	MODEL HAS NOT REACHED CENTERLINE									
3613	MODEL HAS NOT REACHED CENTERLINE									
INJECT TIME =	1.90									
R 5111(685)	2.05	.98	540.0	7.843E-03	9.308E-03	.3604	1.144E-02	1.372E-02	9.920E-03	1.185E-02
T 9425(566)	2.15	1.08	540.0	1.155E-03	1.380E-03	.0534	1.583E-03	1.911E-03	1.409E-03	1.695E-03
B 5112(685)	2.55	1.48	540.0	6.386E-03	7.572E-03	.2933	9.315E-03	1.116E-02	8.077E-03	9.644E-03
T 9426(566)	2.70	1.63	540.0	9.407E-04	1.123E-03	.0435	1.289E-03	1.555E-03	1.148E-03	1.379E-03
S 3614(685)	2.70	1.63	540.0	6.085E-03	7.217E-03	.2795	8.877E-03	1.064E-02	7.697E-03	9.191E-03
B 5113(685)	3.05	1.98	540.0	5.522E-03	6.552E-03	.2537	8.056E-03	9.656E-03	6.985E-03	8.344E-03
T 9427(566)	3.20	2.13	540.0	8.231E-04	9.831E-04	.0381	1.128E-03	1.361E-03	1.004E-03	1.208E-03
S 3615(685)	3.20	2.13	540.0	5.325E-03	6.319E-03	.2447	7.768E-03	9.313E-03	6.735E-03	8.047E-03
R 5114(685)	3.60	2.53	540.0	4.884E-03	5.798E-03	.2245	7.128E-03	8.546E-03	6.181E-03	7.384E-03
T 9428(566)	3.70	2.63	540.0	7.409E-04	8.843E-04	.0343	1.015E-03	1.224E-03	9.039E-04	1.086E-03
R 5115(685)	4.10	3.03	540.0	4.465E-03	5.295E-03	.2051	6.514E-03	7.805E-03	5.648E-03	6.744E-03
T 9429(566)	4.25	3.18	540.0	6.739E-04	8.043E-04	.0312	9.234E-04	1.114E-03	8.221E-04	9.881E-04
S 3616(685)	4.25	3.18	540.0	4.359E-03	5.169E-03	.2002	6.359E-03	7.619E-03	5.514E-03	6.584E-03
R 5116(685)	4.60	3.53	540.0	4.137E-03	4.907E-03	.1900	6.034E-03	7.232E-03	5.233E-03	6.249E-03
T 9430(566)	4.75	3.68	540.0	6.264E-04	7.477E-04	.0290	8.584E-04	1.035E-03	7.643E-04	9.184E-04
S 3617(685)	4.75	3.68	540.0	4.059E-03	4.806E-03	.1861	5.911E-03	7.083E-03	5.126E-03	6.120E-03
R 5117(685)	5.10	4.03	540.0	3.879E-03	4.594E-03	.1780	5.649E-03	6.777E-03	4.898E-03	5.857E-03
T 9431(566)	5.25	4.18	540.0	5.879E-04	7.020E-04	.0272	8.055E-04	9.720E-04	7.172E-04	8.625E-04
S 3618(685)	5.25	4.18	540.0	3.802E-03	4.512E-03	.1747	5.547E-03	6.650E-03	4.810E-03	5.747E-03
R 5118(685)	5.60	4.53	540.0	3.653E-03	4.335E-03	.1678	5.328E-03	6.389E-03	4.620E-03	5.521E-03
T 9432(566)	5.75	4.68	540.0	5.555E-04	6.629E-04	.0257	7.613E-04	9.179E-04	6.778E-04	8.145E-04
R 5119(685)	6.10	5.03	540.0	3.467E-03	4.117E-03	.1593	5.057E-03	6.067E-03	4.385E-03	5.243E-03
S 3619(685)	6.30	5.23	540.0	3.400E-03	4.035E-03	.1562	4.959E-03	5.947E-03	4.300E-03	5.139E-03
R 5120(685)	6.65	5.58	540.0	3.291E-03	3.905E-03	.1512	4.801E-03	5.756E-03	4.163E-03	4.973E-03
T 9433(566)	6.80	5.73	540.0	5.021E-04	5.997E-04	.0232	6.880E-04	8.303E-04	6.126E-04	7.367E-04
S 3620(685)	6.80	5.73	540.0	3.248E-03	3.854E-03	.1492	4.738E-03	5.681E-03	4.108E-03	4.909E-03

H(TO)

46% > H(TO)

26% > H(TO)

Fig. 4 Printout of Parameters Stored on "Tunnel Tape"

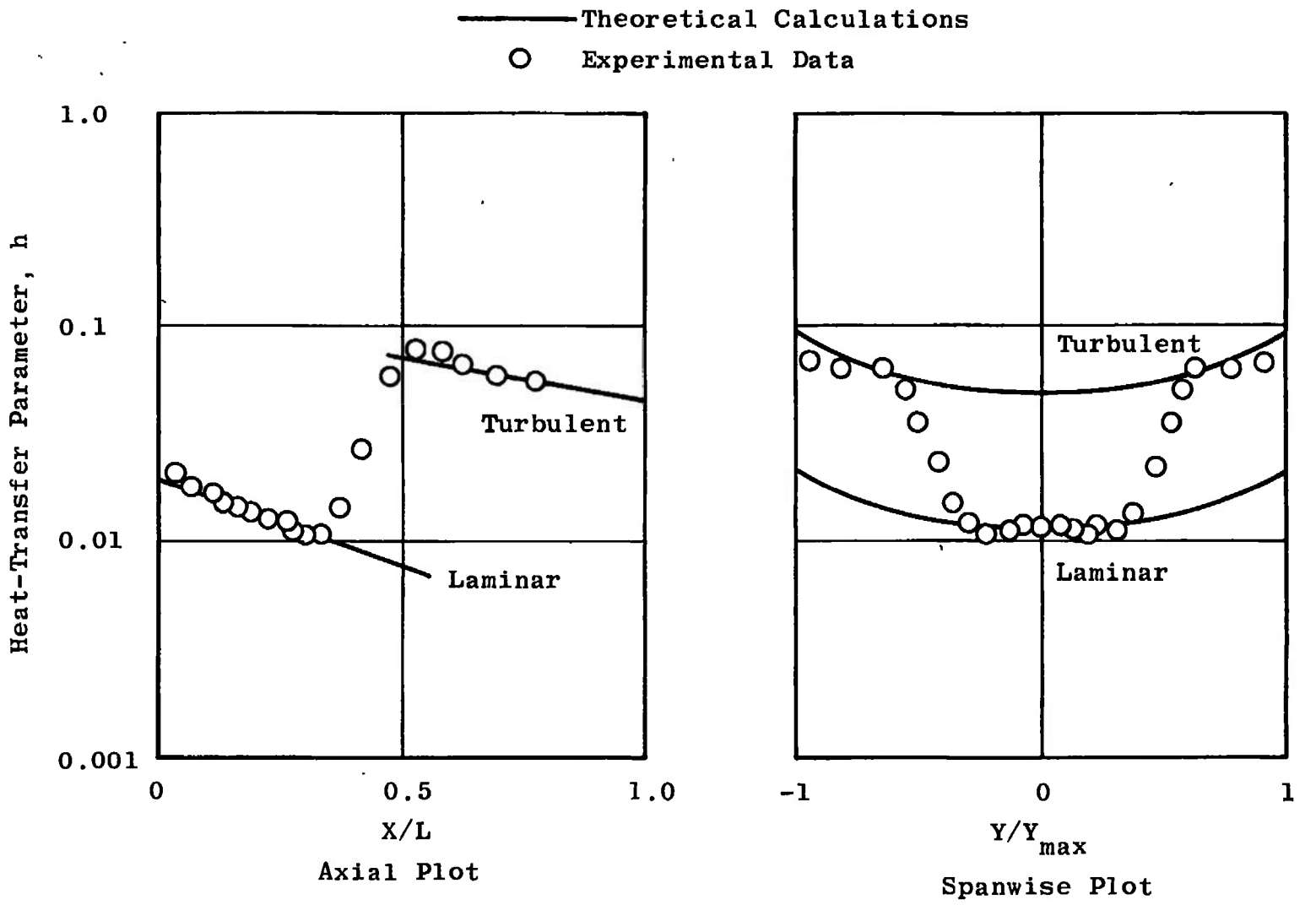

Fig. 5 Illustration of Desired Type of Plots from Phase-Change Paint Test

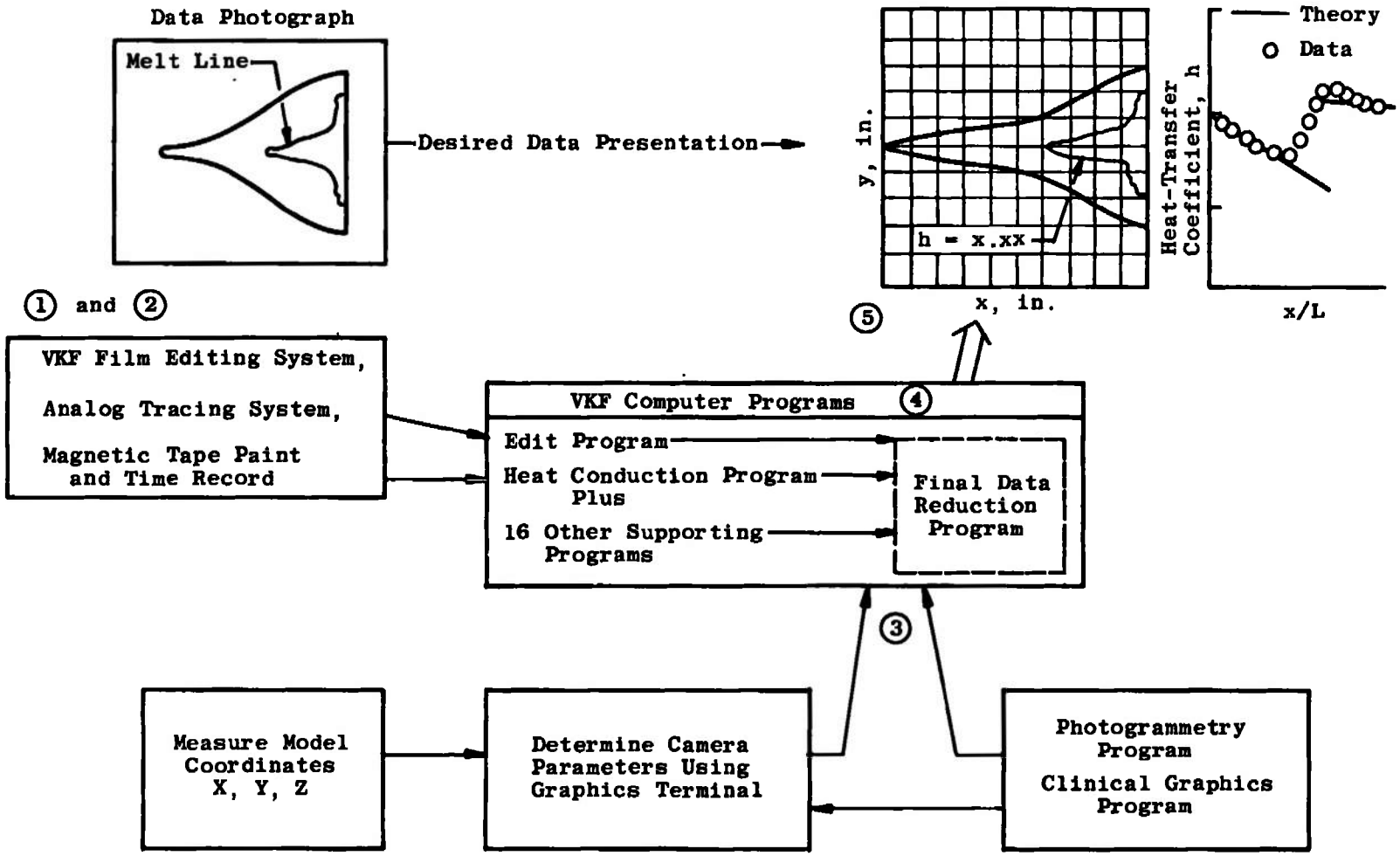

Fig. 6 Schematic Illustrating Reduction of Photographs to Useful Heat-Transfer Parameters

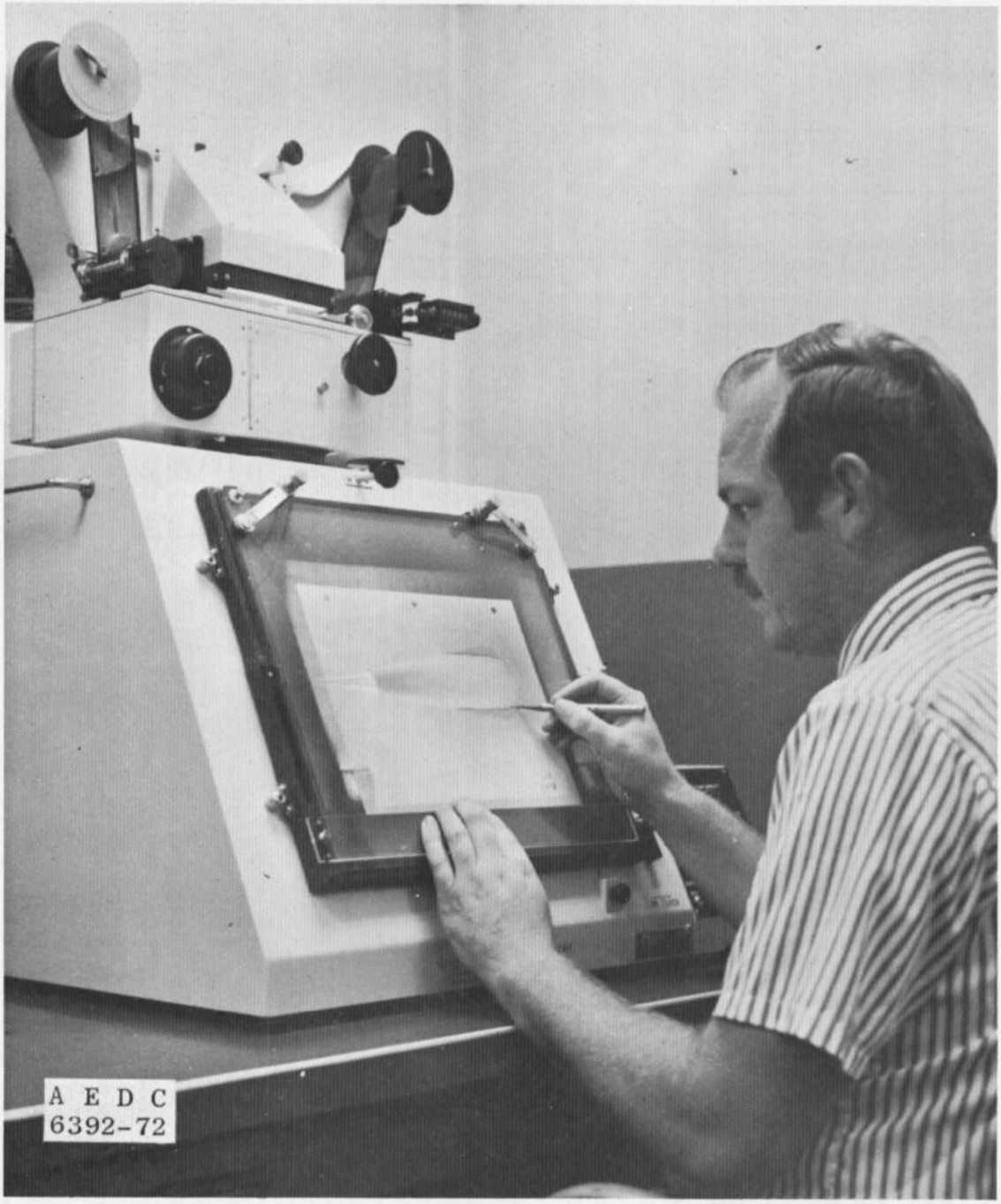

Fig. 7 VKF Film Editing System

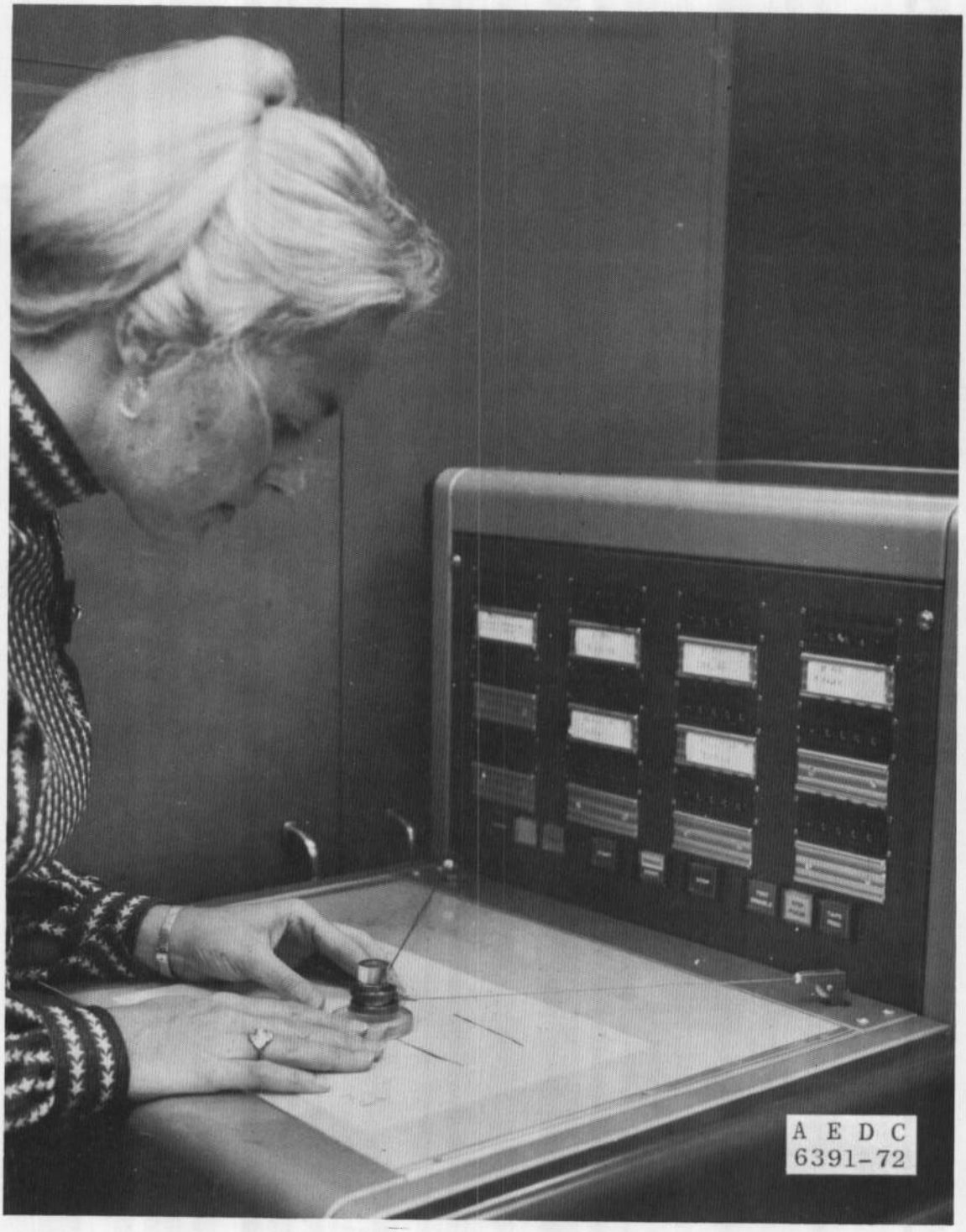

Fig. 8 VKF Analog Tracing System

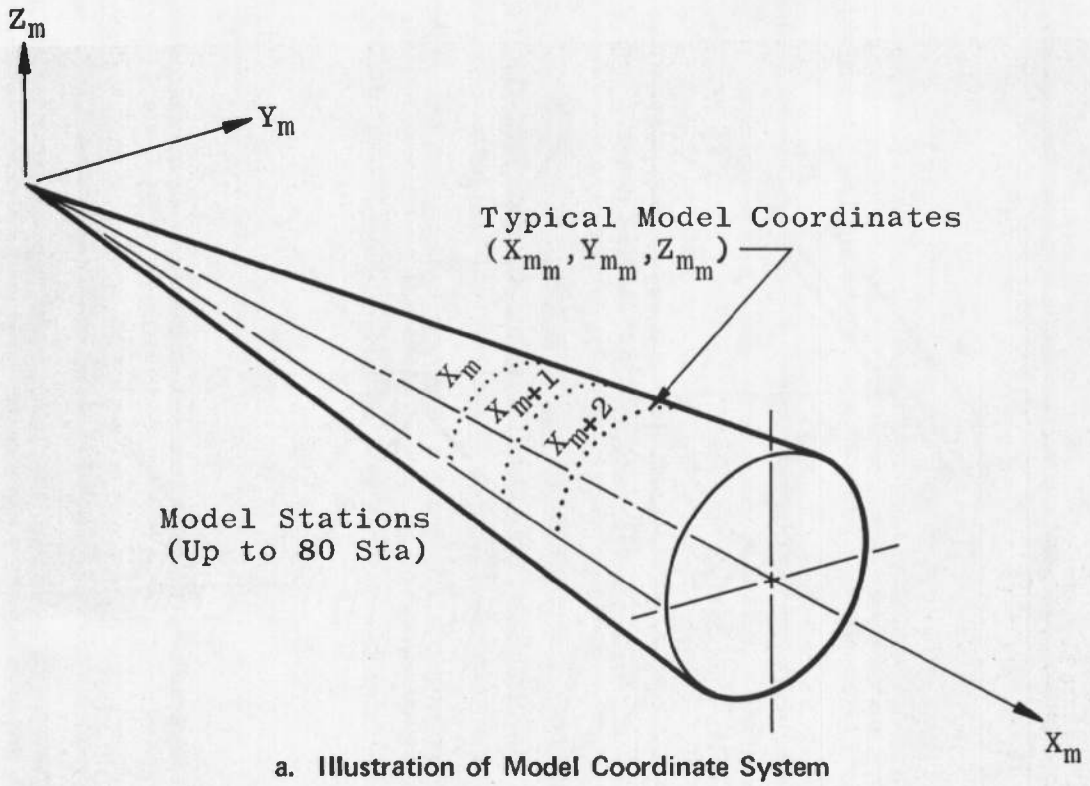

a. Illustration of Model Coordinate System

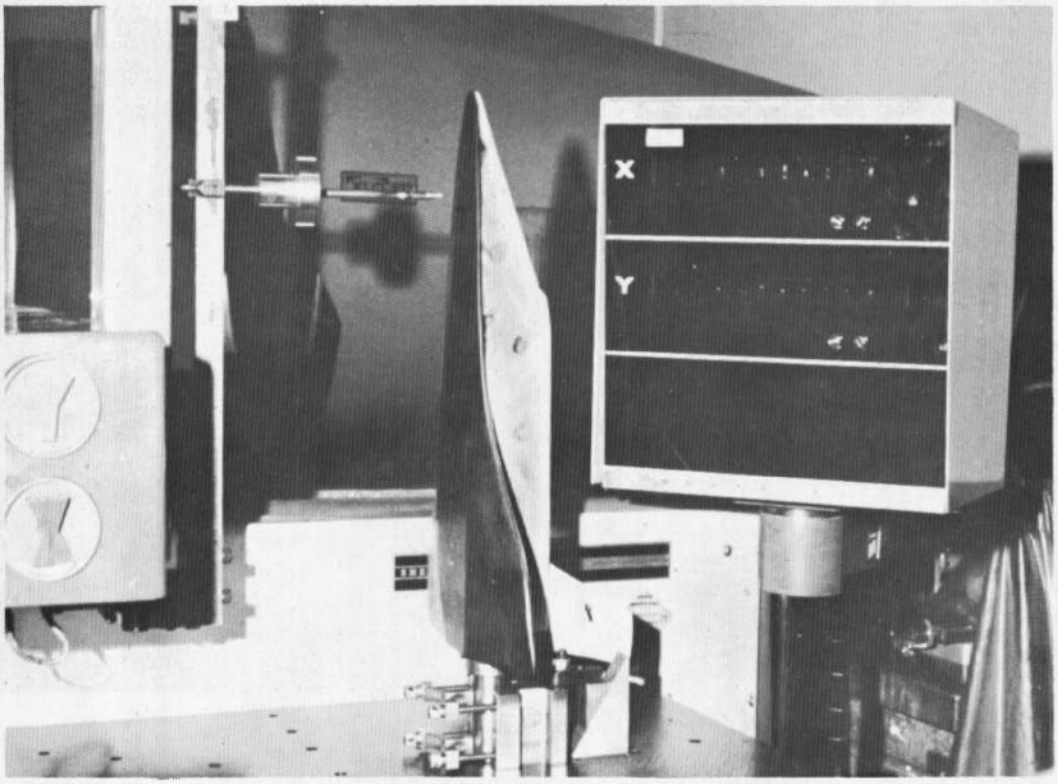

b. Sheffield Cordax Coordinate Measuring Machine

Fig. 9 Model Surface Coordinate Measurement Technique

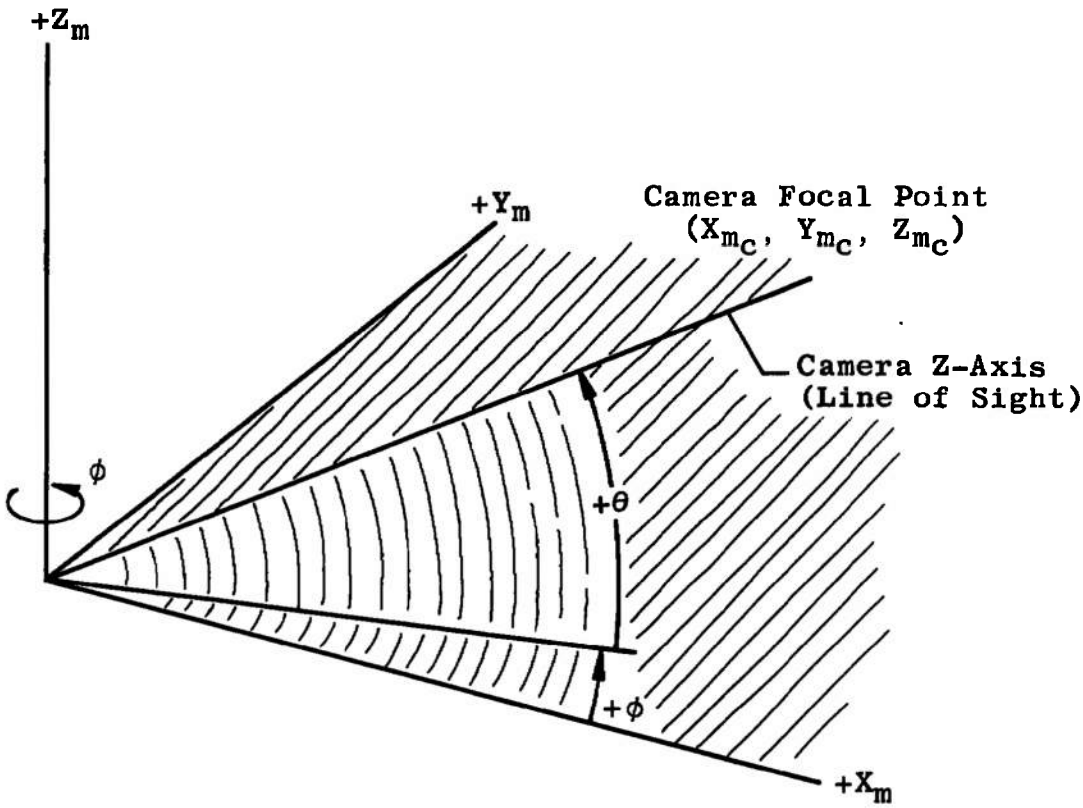

Fig. 10 Sketch Illustrating Rotation Angles

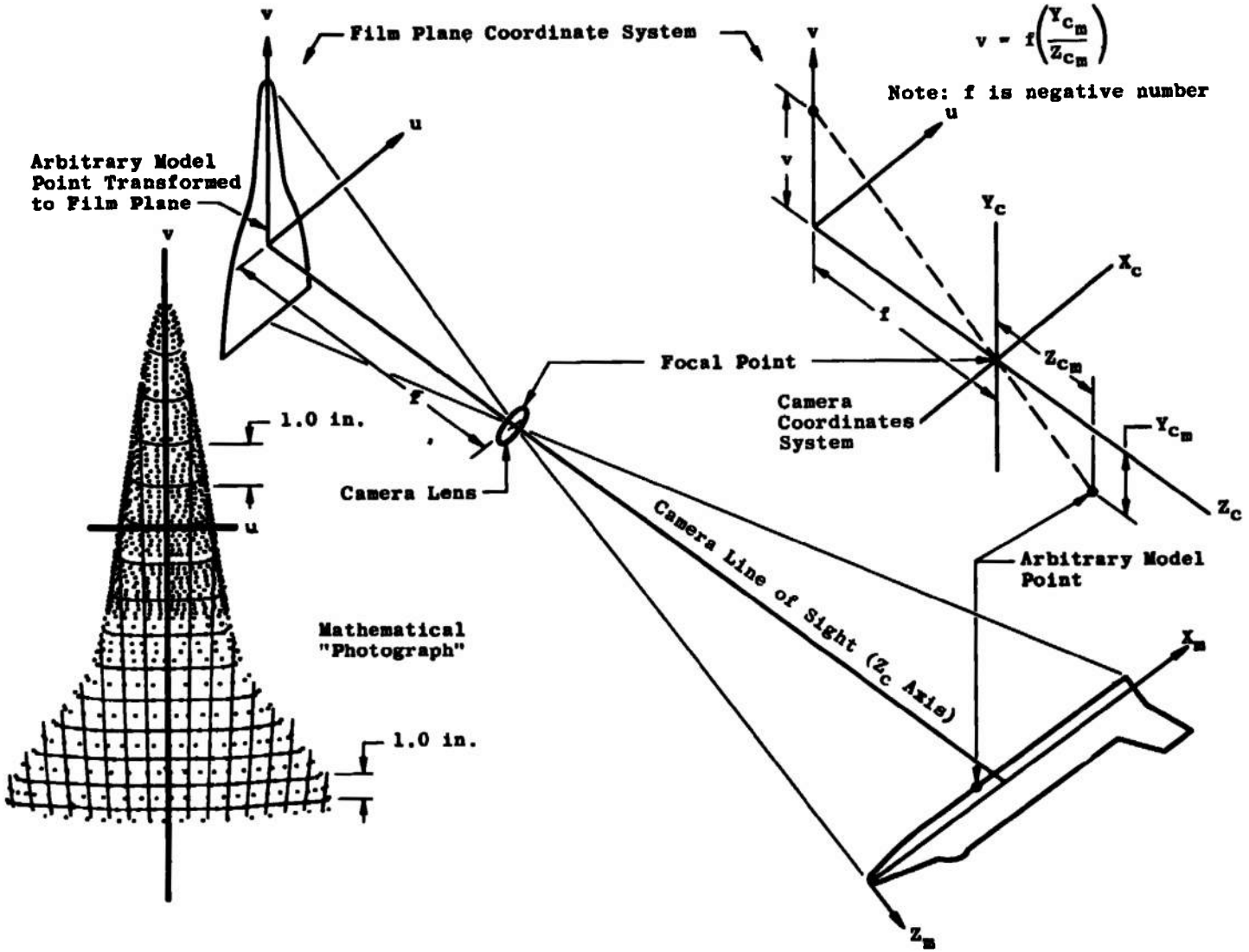

Fig. 11 Sketch Illustrating the Transformation of a Model Surface to the Film Plane

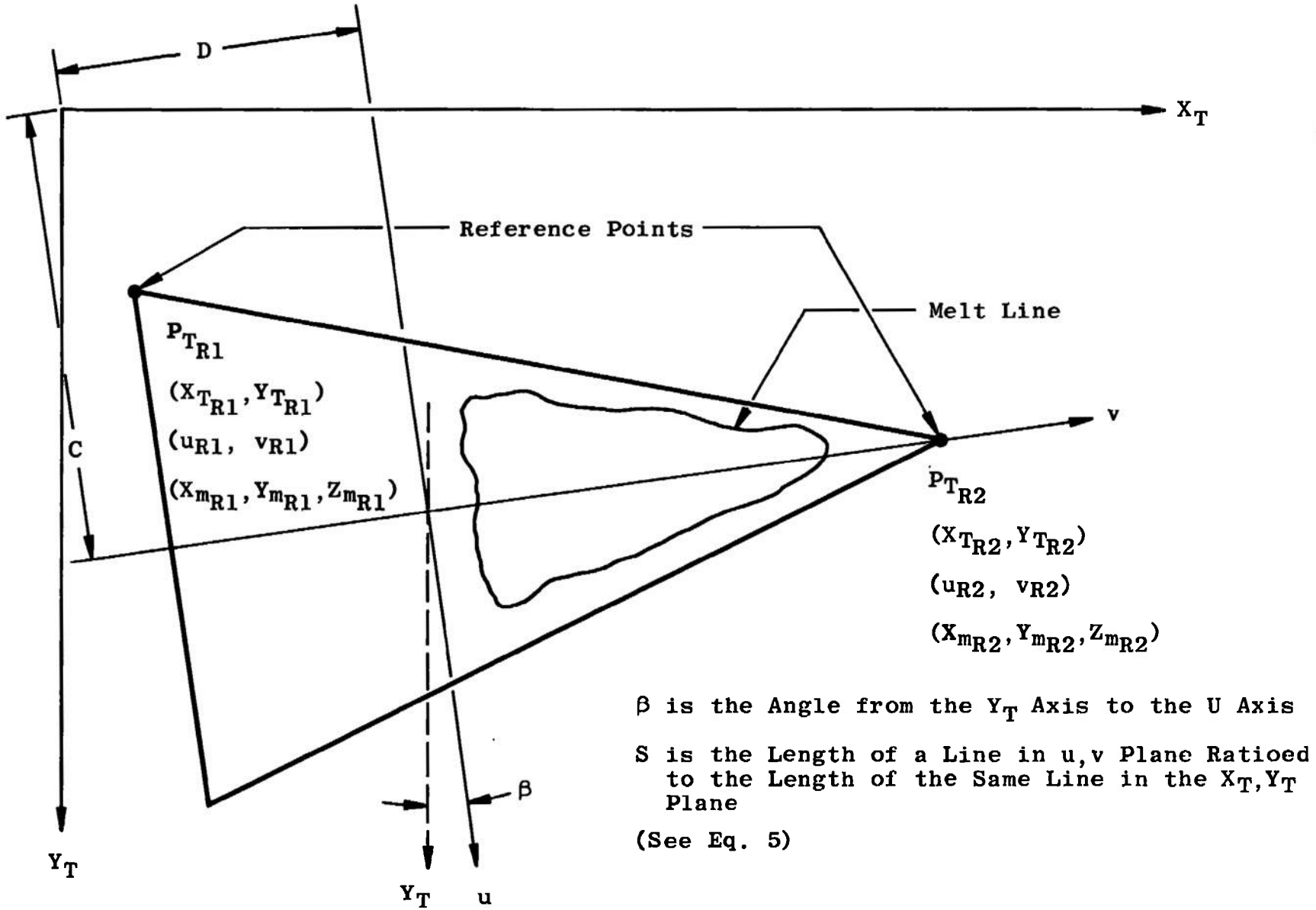

β is the Angle from the Y_T Axis to the U Axis

S is the Length of a Line in u,v Plane Ratioed to the Length of the Same Line in the X_T, Y_T Plane

(See Eq. 5)

Fig. 12 Illustration of Transformation from $X_T Y_T$ Plane to u,v Plane

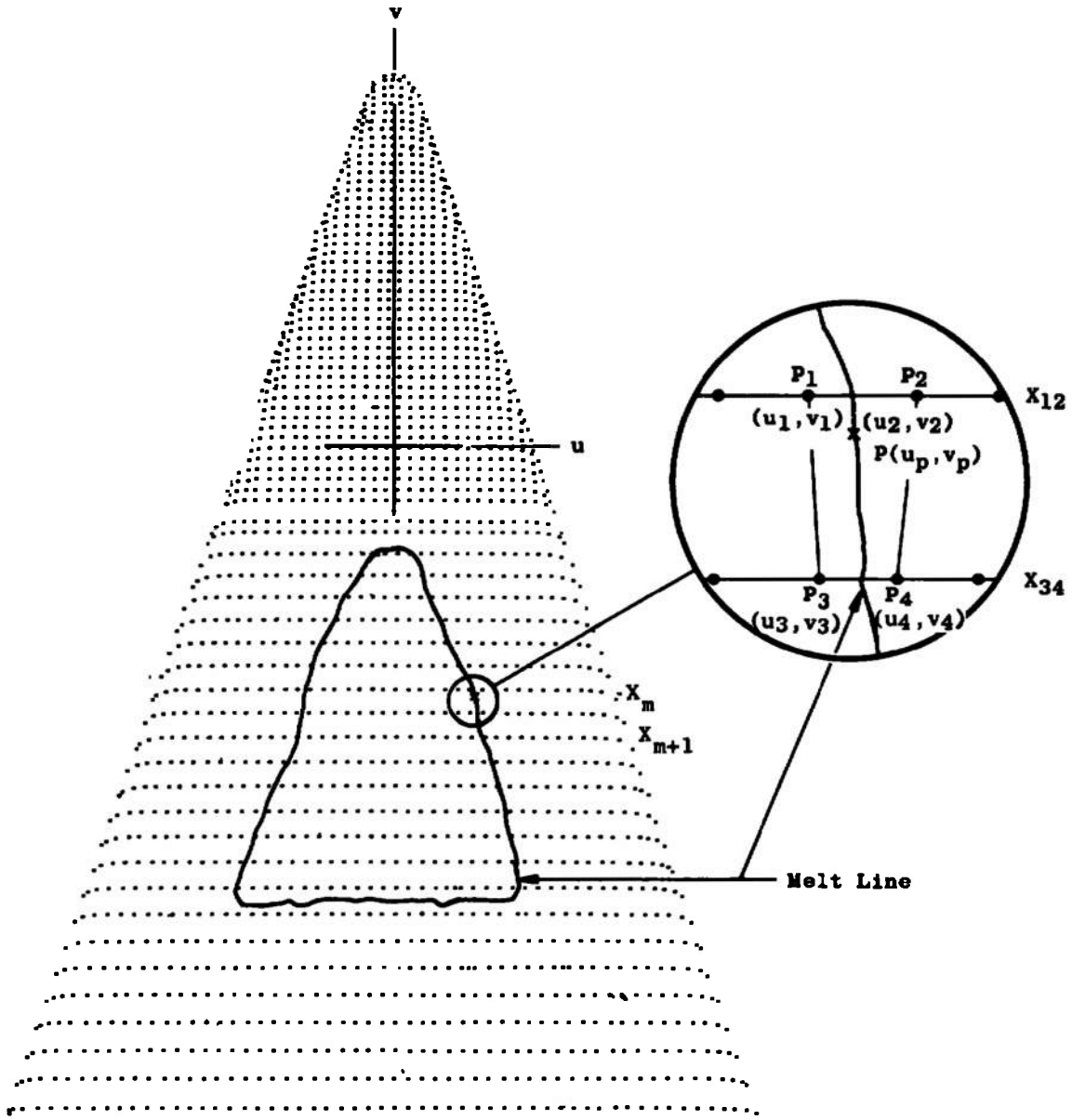

Fig. 13 General Overall Illustration of Interpolation Technique

Note: Known Coordinates For Each Model Point Are (u,v) As Well As the Corresponding Model Coordinates (X_m, Y_m, Z_m)

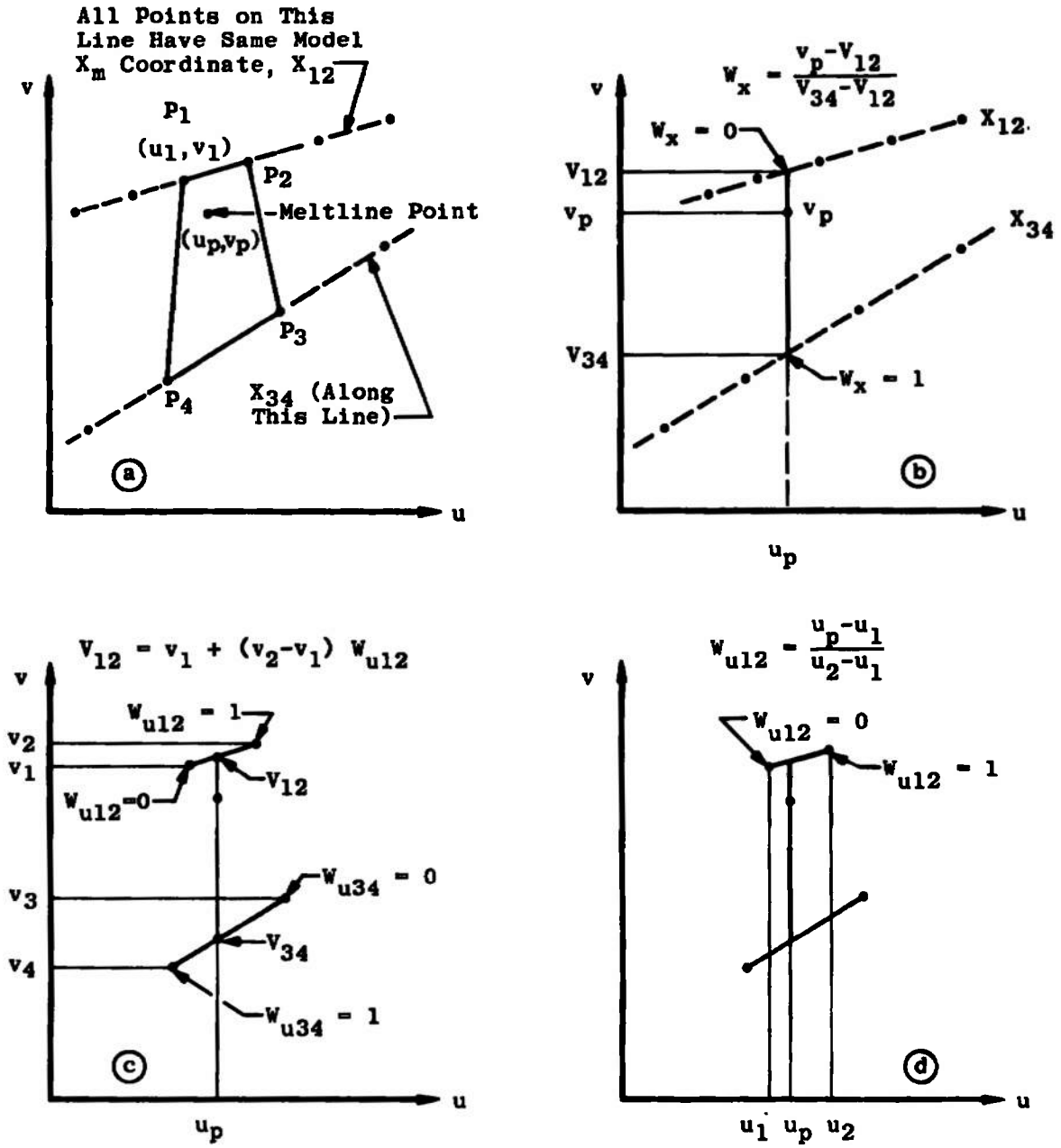

Fig. 14 Details of Interpolation Technique

GROUP	CONFIG	MODEL	MACH NO	PO PSIA	TO DEG R	ALPHA-MODEL	ALPHA-SECTOR	ALPHA-PREBEND	ROLL-MODEL	YAW
.348	11	LNC-UH	4.00	865.9	1343	40.00	10.00	50.00	180.00	-.0

T-INF (DEG R)	P-INF (PSIA)	Q-INF (PSIA)	V-INF (FT/SEC)	RHO-INF (SLUGS/FT3)	MU-INF (LB-SEC/FT2)	RE/FT (FT-1)	HREF (IN= .056FT)	SIREF (IN= .056FT)
97.3	.089	3.924	3847	7.644E-05	2.834E-08	3.17E-06	2.776E-02	1.166E-02

CAMERA	PAINT TEMP (DEG F)	INITIAL TEMP (DEG F)	SQUARE ROOT (HMUACAK)
TOP(1)	400		
SIDE(5)	400	AVERAGE IN = 75	.037
BOTTOM(8)	400		

	PIC NO		TIME	DELTIME	H(TO)	H(TO)/HREF	H(.9TO)	H(.5TO)/HREF	H(.85TO)	H(.85TO)/HREF	S(TO)	MODEL	TEMP F		
T	836	(400)	3.15	2.03	1.39E-02	.5013	1.87E-02	.6749	2.27E-02	.8187	5.773E-03	75	0	75	76
T	837	(400)✓	3.70	2.58✓	1.23E-02	.4446	1.662E-02	.5986	2.016E-02	.7262	5.121E-03✓	76	0	74	76
T	839	(400)	4.75	3.63	1.04E-02	.3749	1.401E-02	.5047	1.699E-02	.6122	4.319E-03	77	0	74	76
T	840	(400)	5.25	4.13	9.75E-03	.3514	1.315E-02	.4731	1.593E-02	.5738	4.048E-03	78	0	74	76
T	842	(400)	6.30	5.18	8.71E-03	.3138	1.17cE-02	.4225	1.422E-02	.5124	3.615E-03	81	0	75	76
T	844	(400)	7.35	6.23	7.94E-03	.2862	1.069E-02	.3854	1.297E-02	.4675	3.294E-03	85	0	76	76
T	851	(400)	11.05	9.93	6.29E-03	.2266	8.467E-03	.3051	1.027E-02	.3700	2.609E-03	103	0	79	79
T	860	(400)	15.80	14.68	5.17E-03	.1864	6.960E-03	.2509	8.447E-03	.3044	2.146E-03	128	0	88	84

a. Tabulated Parameters

Fig. 15 Data Presentation of a Typical Run

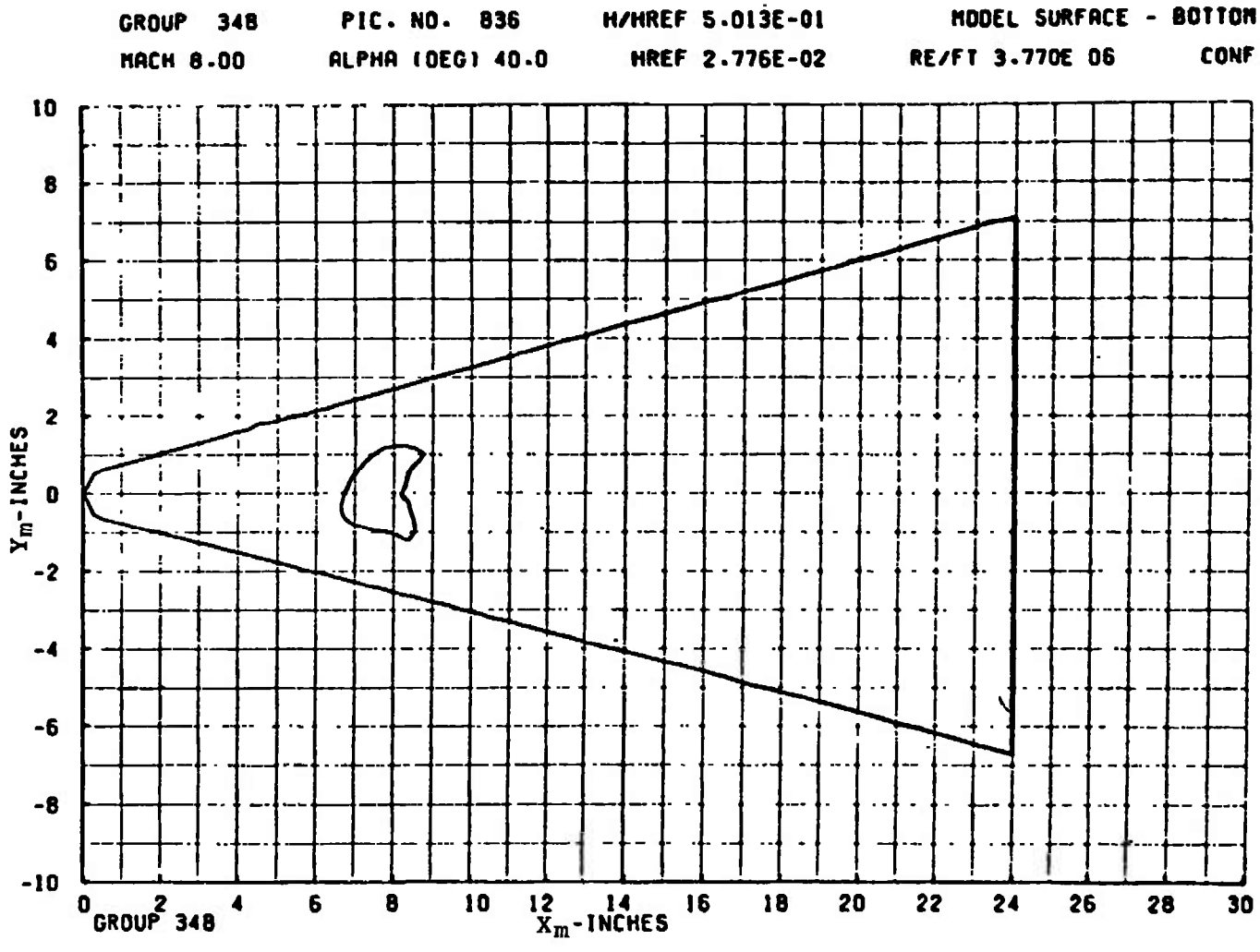

b. Melt Line Contour for H/HREF = 5.013E-01
Fig. 15 Continued

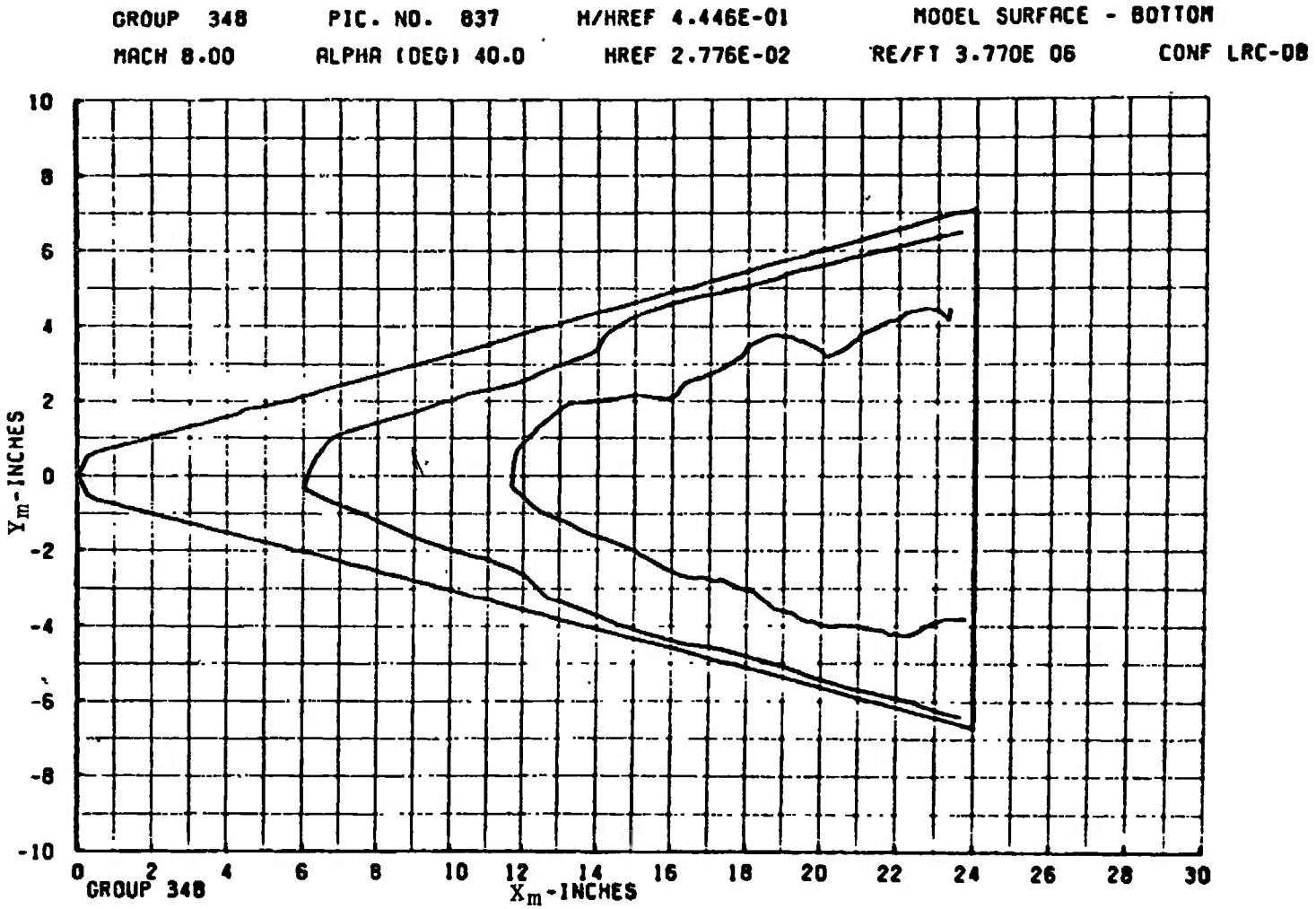

c. Melt Line Contour for H/HREF = 4.446E-01
Fig. 15 Continued

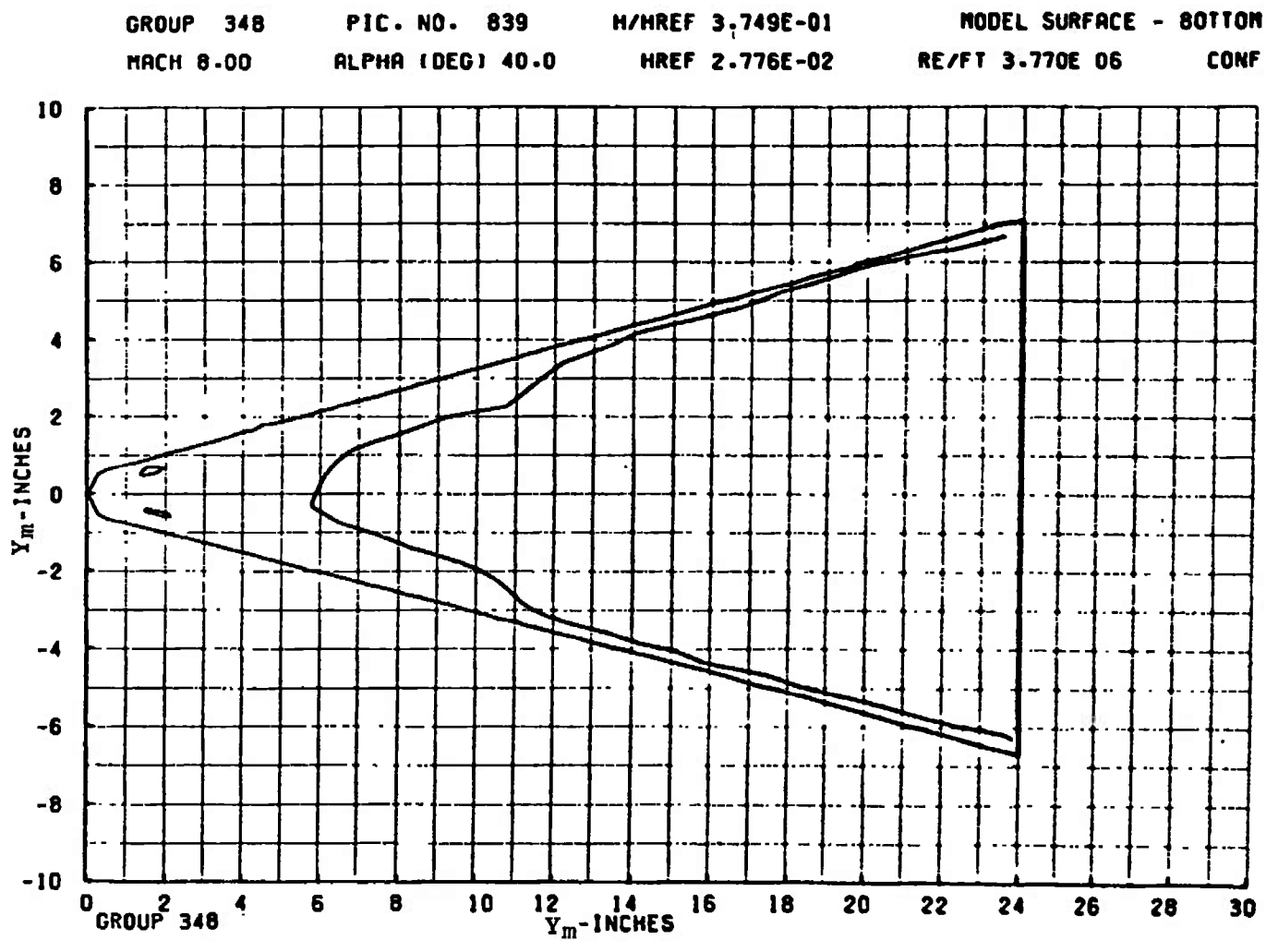

d. Melt Line Contour for H/HREF = 3.749E-01
Fig. 15 Continued

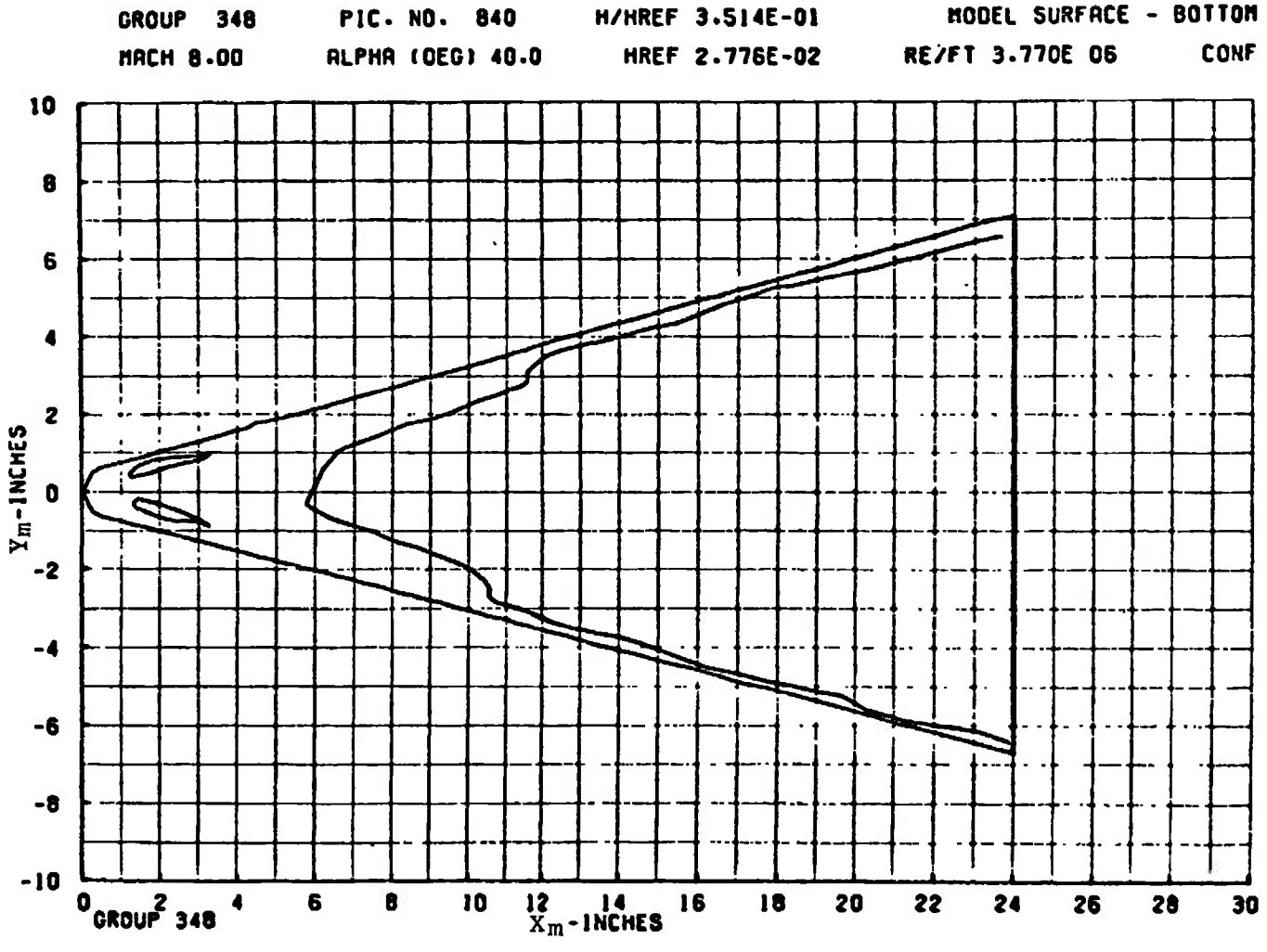

e. Melt Line Contour for H/HREF = 3.514E-01
Fig. 15 Continued

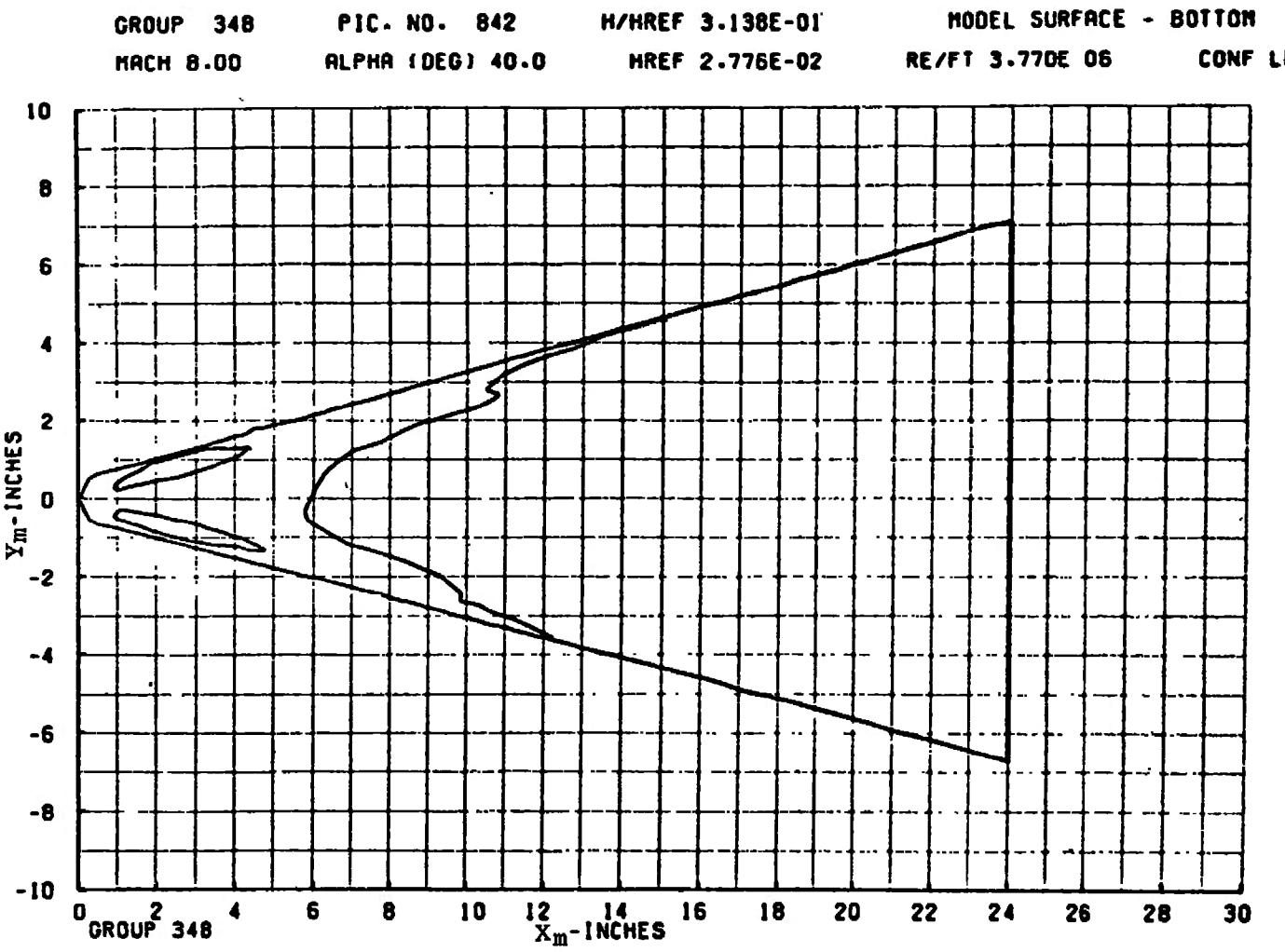

f. Melt Line Contour for H/HREF = 3.138E-01
Fig. 15 Continued

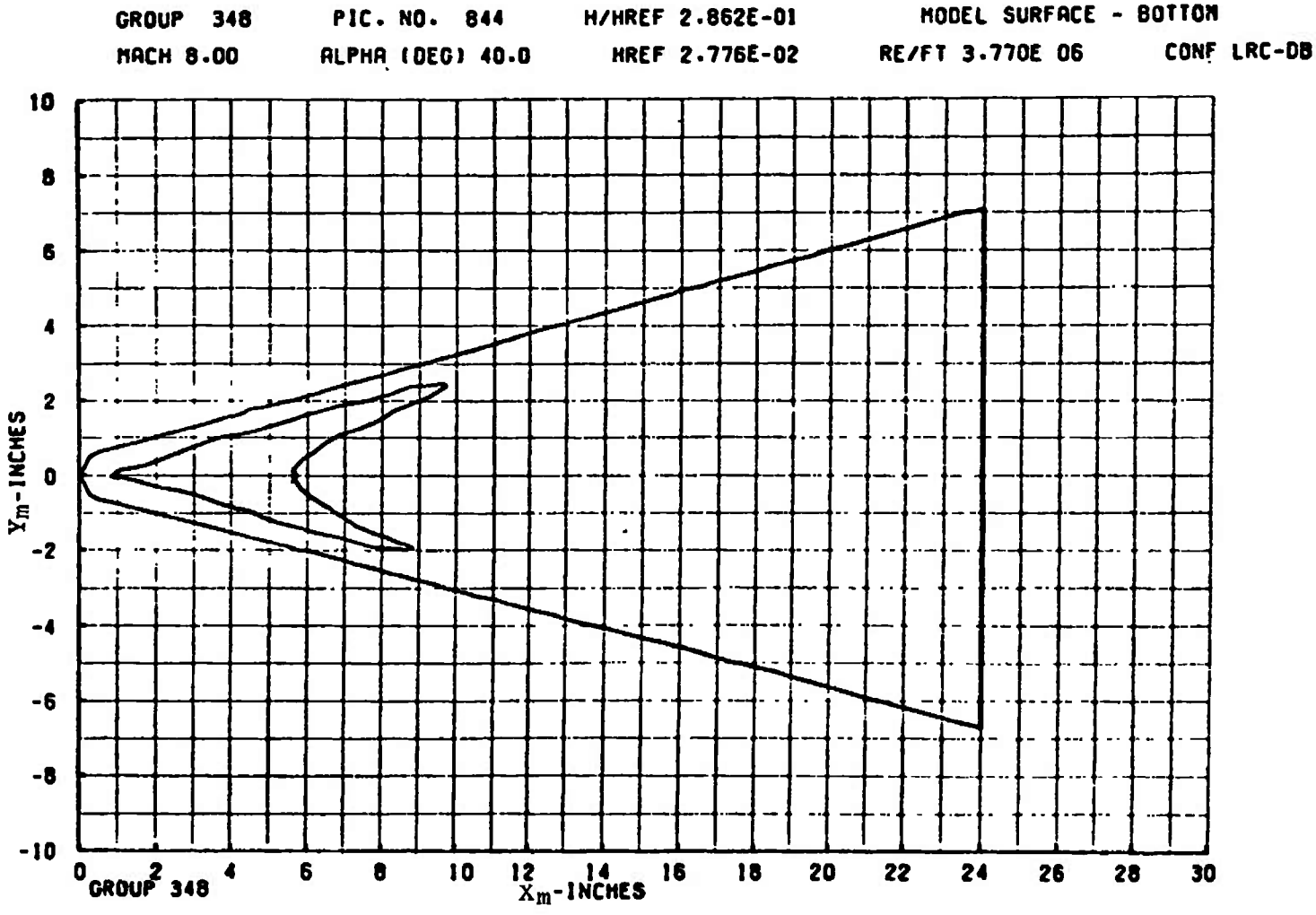

g. Melt Line Contour for H/HREF = 2.862E-01
Fig. 15 Continued

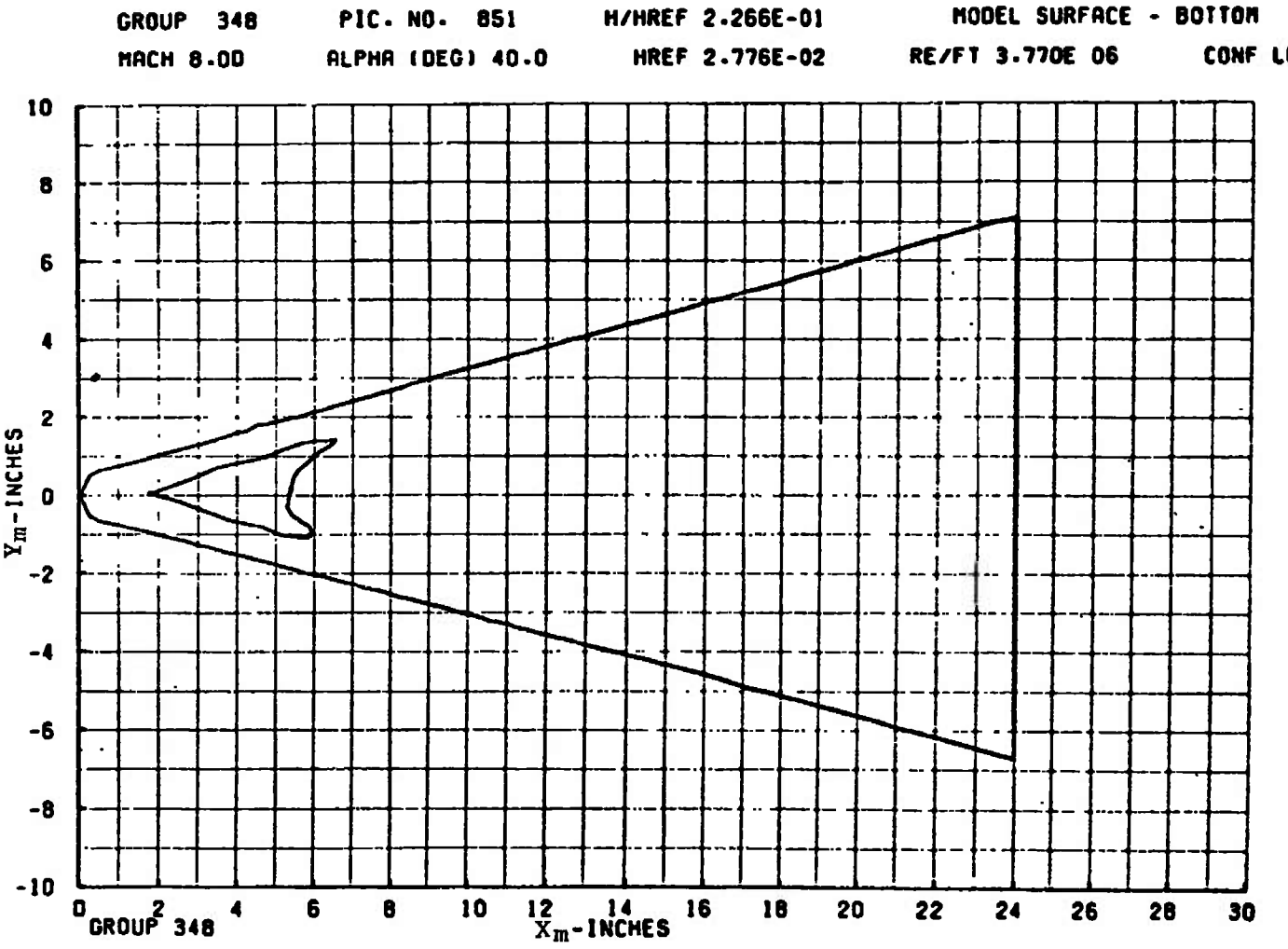

h. Melt Line Contour for H/HREF = 2.266E-01
Fig. 15 Continued

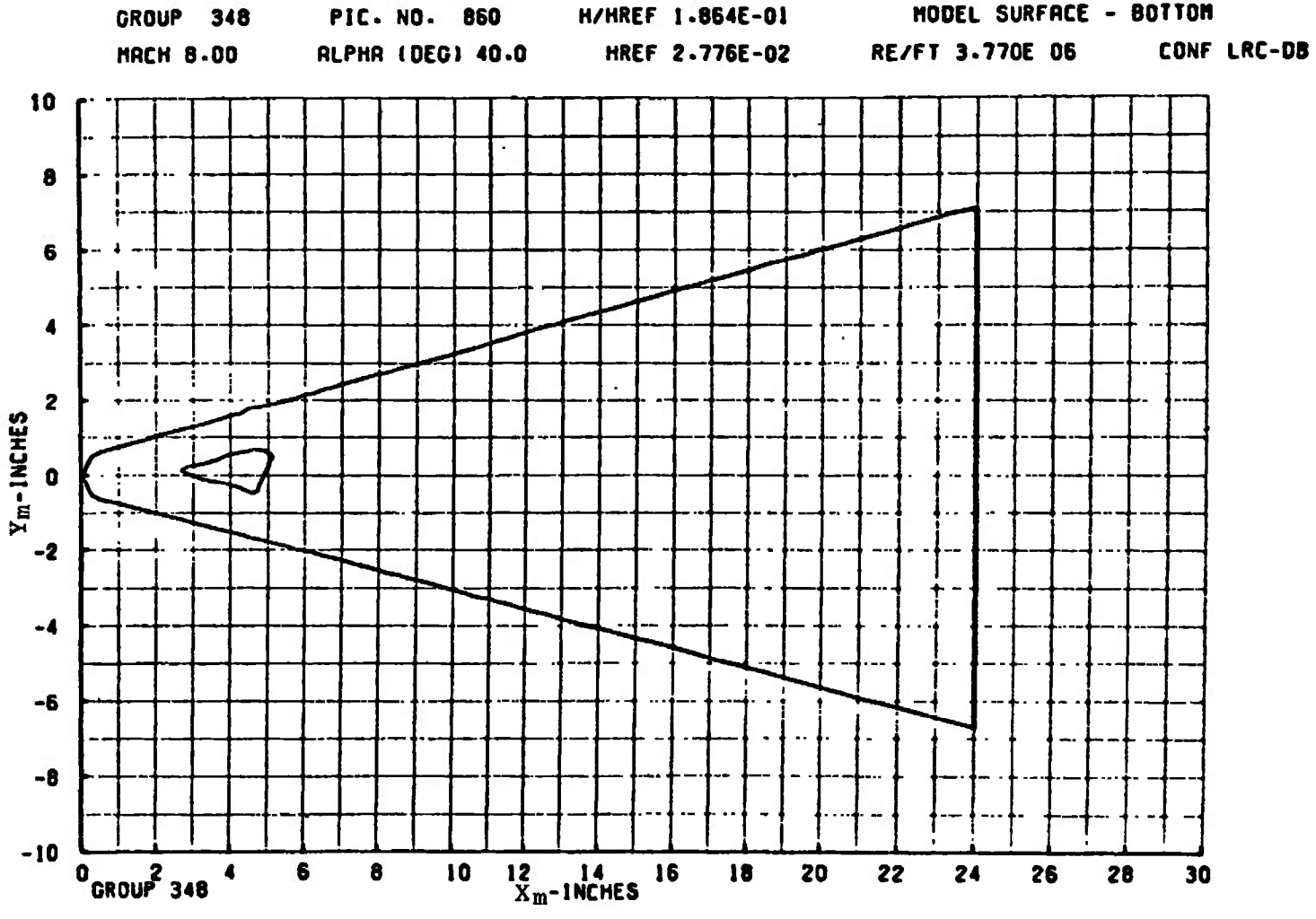

i. Melt Line Contour for H/HREF = 1.864E-01
Fig. 15 Continued

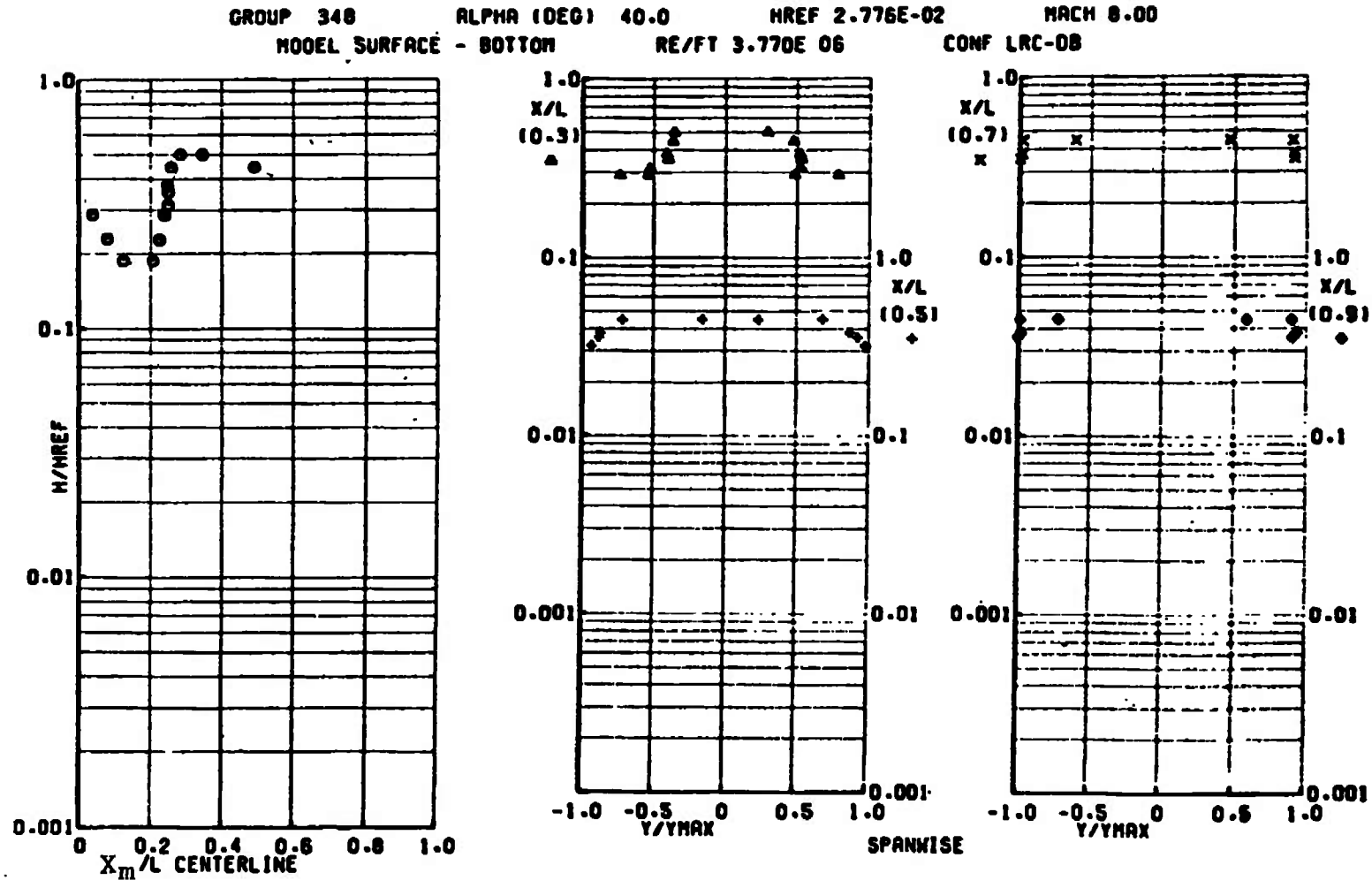

j. Axial and Spanwise Data Plots
Fig. 15 Concluded

UNCLASSIFIED

Security Classification

DOCUMENT CONTROL DATA - R & D

(Security classification of title, body of abstract and indexing annotation must be entered when the overall report is classified)

1 ORIGINATING ACTIVITY *(Corporate author)*
Arnold Engineering Development Center
Arnold Air Force Station, Tennessee 37389

2a. REPORT SECURITY CLASSIFICATION
UNCLASSIFIED

2b GROUP
N/A

3 REPORT TITLE
REDUCTION OF PHOTOGRAPHIC HEAT-TRANSFER RATE DATA AT AEDC

4 DESCRIPTIVE NOTES *(Type of report and inclusive dates)*
July 1971 to September 1972--Final Report

5 AUTHOR(S) *(First name, middle initial, last name)*
R. K. Matthews and G. E. Gilley, ARO, Inc.

6. REPORT DATE	7a. TOTAL NO. OF PAGES	7b. NO. OF REFS
June 1973	44	12

8a. CONTRACT OR GRANT NO

b. PROJECT NO

c. Program Element 64719F

d.

9a. ORIGINATOR'S REPORT NUMBER(S)
AEDC-TR-73-90

9b. OTHER REPORT NO(S) *(Any other numbers that may be assigned this report)*
ARO-VKF-TR-73-33

10 DISTRIBUTION STATEMENT
Approved for public release; distribution unlimited.

11 SUPPLEMENTARY NOTES
Available in DDC

12 SPONSORING MILITARY ACTIVITY
Arnold Engineering Development Center, Air Force Systems Command, Arnold AF Station, Tennessee 37389.

13 ABSTRACT

The development of the phase-change paint technique has provided access to a wealth of information in the form of photographs of heating rate patterns on wind tunnel test models. However, difficulty is experienced in the transformation of the data from the photographs to model coordinates because of the distortion of the model image caused by oblique camera views. This report documents the unique capabilities recently developed at the AEDC-VKF for transformation of the photographic information into a model axis system and for presentation of the data in machine generated plots.

DD FORM 1 NOV 65 1473

UNCLASSIFIED

Security Classification

14. KEY WORDS	LINK A		LINK B		LINK C	
	ROLE	WT	ROLE	WT	ROLE	WT
test facilities						
photographic techniques						
computer programs						
heat transfer						
spacecraft						
reentry vehicle						

AFSC
Arnold AFS Tenn